

January 1969

# Analog Computer Simulation of the Runoff Characteristics of an Urban Watershed

V. V. Dhruva Narayana

J. Paul Riley

Eugene K. Israelsen

Follow this and additional works at: [http://digitalcommons.usu.edu/water\\_rep](http://digitalcommons.usu.edu/water_rep)



Part of the [Civil and Environmental Engineering Commons](#), and the [Water Resource Management Commons](#)

---

## Recommended Citation

Dhruva Narayana, V. V.; Riley, J. Paul; and Israelsen, Eugene K., "Analog Computer Simulation of the Runoff Characteristics of an Urban Watershed" (1969). *Reports*. Paper 186.

[http://digitalcommons.usu.edu/water\\_rep/186](http://digitalcommons.usu.edu/water_rep/186)

This Report is brought to you for free and open access by the Utah Water Research Laboratory at DigitalCommons@USU. It has been accepted for inclusion in Reports by an authorized administrator of DigitalCommons@USU. For more information, please contact [becky.thoms@usu.edu](mailto:becky.thoms@usu.edu).



**ANALOG COMPUTER SIMULATION OF THE RUNOFF  
CHARACTERISTICS OF AN URBAN WATERSHED**

by

**V.V. Dhruva Narayana,  
J. Paul Riley,  
and Eugene K. Israelsen**

**The work reported by this project completion report was supported  
in part with funds provided by the Department of the Interior,  
Office of Water Resources Research under P.L. 88-379,  
Project Number-B-016-Utah, Agreement Number-  
14-01-0001-1563, Investigation Period-  
July 1, 1967 to December 31, 1969.**

**Utah Water Research Laboratory  
College of Engineering  
Utah State University  
Logan, Utah 84321**

**PRWG56-1**

January 1969

**\$2.50**



## ACKNOWLEDGMENTS

This publication represents the final report of a project which was supported in part with funds provided by the Office of Water Resources Research of the United States Department of the Interior as authorized under the Water Resources Research Act of 1964, Public Law 88-379. The work was accomplished by personnel of the Utah Water Research Laboratory in accordance with a research proposal which was submitted to the Office of Water Resources Research through the Utah Center for Water Resources Research at Utah State University. This University is the institution designated to administer the programs of the Office of Water Resources Research in Utah.

The authors acknowledge the support provided by Mr. Trigg Twichell and several members of his staff in the Texas District of the Water Resources Division of the U.S. Geological Survey, who willingly provided available data and helpful suggestions pertaining to the Waller Creek and Wilbarger Creek watersheds at Austin, Texas.

Special thanks are extended to Dr. Frank D. Masch, College of Engineering, University of Texas at Austin and to Mr. W. H. Espey, Jr., Tracor, Inc., Austin who contributed much to the success of the study through both their own published work and their many helpful suggestions. Appreciation is also expressed for the assistance of Mr. Charles Morgan, Chief Engineer, Department of Public Works, City of Austin.

V.V. Dhruva Narayana  
J. Paul Riley  
Eugene K. Israelsen

3

3

3

3

3

## **ABSTRACT**

### **ANALOG COMPUTER SIMULATION OF THE RUNOFF**

#### **CHARACTERISTICS OF AN URBAN WATERSHED**

In the synthesis of hydrograph characteristics of small urban watersheds, the distribution of water among the various phases of the runoff process is attempted by the concept of equivalent rural watershed. The urban parameters considered in the study are percentage impervious cover and characteristic impervious length factor. A mathematical model is developed for the equivalent rural watershed with precipitation as input. The hydrograph of outflow is obtained by chronologically deducting the losses due to interception, infiltration, and depression storages from precipitation and then routing through the watershed storage.

This mathematical procedure is programmed on an analog computer and is tested with data from the Waller Creek watershed, at Austin, Texas. In the verification process, watershed coefficients representing interception, infiltration, and depression storage are established by trial and error such that the simulated and observed hydrographs are nearly identical with a high statistical correlation. Sensitivity studies indicate the relative influence of the watershed coefficients on the runoff process. The watershed coefficients determined by model verification for each year of study are related to corresponding urban parameters.

Riley, J. Paul; Narayana, V. V. Dhruva; and Israelsen, Eugene K. ANALOG COMPUTER SIMULATION OF THE RUNOFF CHARACTERISTICS OF AN URBAN WATERSHED

Research Project Technical Completion Report to Office of Water Resources Research, Department of the Interior, December 1968, Washington, D.C., 83 p.

**KEYWORDS**--\*urban hydrology/ simulation/ \*simulation of urban hydrology/ \*hydrologic models/ watershed studies/ hydrology/ hydrologic research/ computer simulation/ \*electronic analog computer/ surface runoff/ precipitation/ \*storm drain design/ \*flood frequency/ \*urban parameters/ urban watershed/ \*runoff characteristics/ equivalent rural watershed/ percentage impervious cover/ characteristic impervious length factor.



## TABLE OF CONTENTS

	Page
 Chapter I	
INTRODUCTION . . . . .	1
Objectives . . . . .	1
Organization of the Study . . . . .	1
Review of Literature . . . . .	1
Runoff processes . . . . .	2
Overland and channel flow routing . . . . .	3
Method of storage routing . . . . .	3
Method of solving continuity and momentum equations . . . . .	5
Urban watershed modeling . . . . .	6
Analog computer application . . . . .	8
 Chapter II	
DEVELOPMENT OF THE PHYSICAL MODEL . . . . .	9
Modeling Procedure . . . . .	9
Urban Parameters . . . . .	9
Equivalent Rural Watershed . . . . .	10
Determination of Rainfall Excess . . . . .	11
Precipitation . . . . .	11
Interception . . . . .	11
Infiltration . . . . .	12
Surface depression storage . . . . .	12
Hydrograph of rainfall excess . . . . .	13
Overland and Channel Flow Routing . . . . .	13
 Chapter III	
DESCRIPTION OF THE EXPERIMENTAL WATERSHED . . . . .	17
Climate . . . . .	17
Geology . . . . .	17
Topography . . . . .	17
Instrumentation . . . . .	18
Drainage Conditions . . . . .	18
Urban Parameters . . . . .	18
Percentage impervious cover . . . . .	20
Characteristic impervious length factor . . . . .	20



## Chapter IV

ANALOG COMPUTER PROGRAMMING . . . . .	27
Precipitation . . . . .	28
Interception . . . . .	28
Infiltration . . . . .	29
Depression Storage . . . . .	29
Routing the Rainfall Excess . . . . .	29
Time Scaling . . . . .	29
Amplitude Scaling . . . . .	30
Interception . . . . .	31
Infiltration . . . . .	31
Depression storage . . . . .	31
Routing of rainfall excess . . . . .	31
Outflow rate . . . . .	31
Total volume of outflow . . . . .	32

## Chapter V

MODEL VERIFICATION . . . . .	35
Geometric Characteristics of the Watershed . . . . .	35
Physical Characteristics of the Watershed . . . . .	35
Urban Parameters . . . . .	38
Model Testing . . . . .	38
Watershed Coefficients . . . . .	38
Actual values for each storm . . . . .	38
Average annual values . . . . .	38

## Chapter VI

MODELING RESULTS . . . . .	45
Relation Between Watershed Coefficients and Urban Parameters . . . . .	45
Interception storage capacity . . . . .	45
Maximum and minimum capacity rates . . . . .	45
Depression storage capacity . . . . .	47
Rise time of the unit hydrograph . . . . .	47
Adequacy of the regression equations . . . . .	56
Sensitivity Analyses . . . . .	58
Actual watershed coefficients . . . . .	58
Minimum capacity infiltration rate . . . . .	60
Maximum capacity infiltration rate . . . . .	61
Interception storage capacity . . . . .	61
Depression storage capacity . . . . .	61
Rise time of the unit hydrograph . . . . .	62
General comments . . . . .	63

## Chapter VII

SUMMARY AND CONCLUSIONS . . . . .	69
Summary . . . . .	69
Conclusions . . . . .	70
Recommendations . . . . .	71
LITERATURE CITED . . . . .	73
APPENDIX A . . . . .	75
APPENDIX B . . . . .	79

## LIST OF FIGURES

Figure	Page
1.1 Schematic representation of small watershed model for runoff hydrograph synthesis . . . . .	2
2.1 Schematic sketch illustrating characteristic impervious length . . . . .	9
2.2 Typical actual infiltration rate curve . . . . .	12
3.1 Map of Austin, Texas showing location of Waller Creek watershed . . . . .	17
3.2 Instrumentation of Waller Creek watershed . . . . .	18
3.3 Waller Creek watershed with subunits . . . . .	19
3.4 Urbanization in subunit 29 during the years 1951, 1958, and 1964 . . . . .	20
3.5 Urbanization in subunit 30 during the years 1951, 1958, and 1964 . . . . .	21
3.6 Urbanization in subunit 31 during the years 1951, 1958, and 1964 . . . . .	21
3.7 Yearly variation of percentage impervious cover . . . . .	24
3.8 Yearly variation of characteristic impervious length . . . . .	24
4.1 Analog computer program for outflow hydrograph from equivalent rural watershed . . . . .	27
4.2 Analog circuit for generating the expression for interception rate . . . . .	30

<b>Figure</b>	<b>Page</b>
4.3 Analog circuit for generating the expression for infiltration rate . . . . .	30
4.4 Analog circuit for generating the expression for inflow rate in to depression storage . . . . .	32
4.5 Analog circuit for obtaining the outflow hydrograph . . . . .	32
5.1 Variation of characteristics of unit hydrograph and equivalent rural watershed of 23rd Street with urban parameters, $L_f$ , $C_f$ . . . . .	36
5.2 Variation of characteristics of unit hydrograph and equivalent rural watershed of 38th Street with urban parameters, $L_f$ , $C_f$ . . . . .	37
5.3 Comparison between the simulated and actual hydrographs . . . . .	39
5.4 Comparison of the simulated and actual values of peak rate of outflow . . . . .	43
5.5 Comparison of the simulated and actual values of the rise time of the hydrograph . . . . .	43
5.6 Comparison of the simulated and actual values of the total volume of outflow . . . . .	43
5.7 Comparison of the simulated and actual values of total duration of the hydrograph . . . . .	43
6.1 The relationship between the actual and the estimated interception storage capacity . . . . .	45
6.2 The relationship between the actual and the estimated maximum infiltration capacity rates . . . . .	55
6.3 The relationship between the actual and estimated minimum infiltration capacity rates . . . . .	56
6.4 The relationship between the actual and the estimated depression storage capacity . . . . .	58
6.5 The relationship between the actual and the estimated risetime of the unit hydrograph . . . . .	58
6.6 Outflow hydrographs resulting from the variation of $f_o$ for the storm on 1 May 1956 . . . . .	60
6.7 Outflow hydrographs resulting from the variation of $f_o$ for the storm on 26 May 1957 . . . . .	60
6.8 Variation in the ratios of the peak rate and total volume of outflow corresponding to the variation in the maximum infiltration capacity . . . . .	61
6.9 Outflow hydrographs resulting from the variation of $f_c$ for the storm on 1 May 1956 . . . . .	63
6.10 Outflow hydrographs resulting from the variation of $f_c$ for the storm on 26 May 1957 . . . . .	63
6.11 Variation of the peak rate and total volume of outflow corresponding to the variation in the minimum infiltration capacity . . . . .	64

Figure	Page
6.12 Outflow hydrographs resulting from the variation of $S_I$ for the storm on 1 May 1956 . . . . .	64
6.13 Outflow hydrographs resulting from the variation of $S_I$ for the storm on 26 May 1957 . . . . .	65
6.14 Variation of the peak rate and total volume of outflow corresponding to the variation in the interception storage capacity . . . . .	65
6.15 Outflow hydrographs resulting from the variation of depression storage capacity on 1 May 1956 . . . . .	65
6.16 Outflow hydrographs resulting from the variation of depression storage capacity on 26 May 1957 . . . . .	66
6.17 Variation of the peak rate and total volume of outflow corresponding to the variation in depression storage capacity . . . . .	66
6.18 Outflow hydrographs resulting from the variation of the risetime of the unit hydrograph for the storm on 1 May 1956 . . . . .	66
6.19 Outflow hydrographs resulting from the variation of the rise time of the unit hydrograph for the storm on 26 May 1957 . . . . .	67
6.20 Variation in the peak rate of flow corresponding to the variation in the rise time of the unit hydrograph . . . . .	68

## LIST OF TABLES

Table	Page
2.1 Equations for unit hydrograph characteristics . . . . .	10
3.1 Geometric particulars of Waller Creek watershed . . . . .	18
3.2 Impervious areas in the subunits . . . . .	22
3.3 Characteristic impervious lengths ( $l_i$ ) . . . . .	23
3.4 Chronological development of urbanization . . . . .	25
4.1 Scale factors relating the physical and computer variables . . . . .	33
5.1 Characteristics of simulated and actual outflow hydrograph for the Waller Creek watershed . . . . .	40
5.2 Regression between actual and simulated hydrograph characteristics . . . . .	42
6.1 Urban parameters and physical characteristics of the equivalent rural watersheds of Waller Creek urban catchments . . . . .	46
6.2 Urban parameters and average annual physical characteristics of the equivalent rural watersheds of Waller Creek urban catchments . . . . .	47
6.3 Coefficients of regression for various models relating interception storage with the urban parameters . . . . .	48

<b>Table</b>	<b>Page</b>
6.4 Analysis of variance for interception storage capacity, related to the urban parameters by model 1 . . . . .	48
6.5 Analysis of variance for interception storage capacity, related to the urban parameters by the model 2 . . . . .	48
6.6 Comparison of the actual and estimated values of interception storage capacity . . . . .	49
6.7 Linear correlation of maximum and minimum infiltration capacities with the urban parameters . . . . .	50
6.8 Analysis of variance for relating maximum infiltration capacity rate with the urban parameters . . . . .	50
6.9 Analysis of variance for relating minimum infiltration capacity rate with the urban parameters . . . . .	50
6.10 Comparison of the actual and estimated maximum infiltration capacity rates . . . . .	51
6.11 Comparison of the actual and the estimated minimum infiltration capacity rates . . . . .	52
6.12 Coefficients of regression for various models relating depression storage capacity with the urban parameters . . . . .	53
6.13 Analysis of variance for depression storage capacity related to the urban parameters by the model 1 . . . . .	53
6.14 Analysis of variance for depression storage capacity related to the urban parameters by the model 2 . . . . .	53
6.15 Comparison of the actual and the estimated depression storage capacity . . . . .	54
6.16 Analysis of variance for relating the rise time of the unit hydrograph with the urban parameters . . . . .	56
6.17 Comparison between the actual and the estimated values of rise time of the unit hydrograph . . . . .	57
6.18 Values of urban parameters for the watershed . . . . .	59
6.19 Watershed coefficients for rural and urban watersheds . . . . .	59
6.20 Actual values of the watershed coefficients . . . . .	60
6.21 Maximum infiltration capacity and peak rate and total volume of outflow . . . . .	62
6.22 Minimum infiltration capacity and peak rate and total volume of outflow . . . . .	63
6.23 Interception storage capacity and peak rate and total volume of outflow . . . . .	64
6.24 Depression storage capacity and the peak rate and total volume of outflow . . . . .	67
6.25 Rise time of the unit hydrograph and peak rate of outflow . . . . .	67

## PARTIAL LIST OF SYMBOLS <sup>1</sup>

Symbol	Definition
A	watershed area
C	Izzard's roughness factor
C <sub>f</sub>	percentage impervious cover
E	rate of evaporation
F	mass infiltration
H	elevation difference between the highest point and the runoff gage location on a watershed
I	average intensity of precipitation
I <sub>c</sub>	total interception volume at any instant expressed as the mean depth of the watershed
L	maximum length of travel on the watershed
L <sub>ER</sub>	length of travel on the equivalent rural watershed
L <sub>f</sub>	characteristics impervious length factor
L <sub>m</sub>	mean characteristic impervious length
P	mass rainfall
P <sub>1</sub>	mass net precipitation
Q	rate of surface runoff for a storm
Q <sub>o</sub>	soil moisture index
Q <sub>p</sub>	peak rate of outflow
Q <sub>T</sub>	total volume of outflow
S	storage
S <sub>o</sub>	slope of the channel bed
S <sub>c</sub>	slope of a reach along a flow path
S <sub>D</sub>	depression storage capacity expressed as mean depth for the watershed
S <sub>ER</sub>	slope of the equivalent rural watershed
S <sub>f</sub>	slope of the energy line
S <sub>I</sub>	volume of interception storage capacity expressed as average depth for the watershed
T	storm duration
T <sub>M</sub>	average storage delay time
T <sub>R</sub>	rise time of the actual hydrograph
V <sub>d</sub>	volume of water stored in surface depressions at any instant
c	parameter characterizing the porosity of the upper soil layer
d	moisture deficiency
e	exponential base
f	capacity infiltration rate
f <sub>o</sub>	maximum capacity infiltration rate
f <sub>a</sub>	actual infiltration rate
f <sub>c</sub>	minimum capacity infiltration rate
f <sub>t1</sub>	initial capacity infiltration rate
g	acceleration due to gravity
i	rainfall intensity
i <sub>o</sub>	average rainfall intensity during a storage delay period
i <sub>1</sub>	net precipitation rate

<sup>1</sup>Symbols not included in this list are defined within the text of the report.

## PARTIAL LIST OF SYMBOLS (Continued)

Symbol	Definition
$i_2$	rate of outflow after losses due to interception and infiltration are deducted from rainfall $i$
$i_{ca}$	actual interception rate
$i_{cc}$	capacity interception rate
$k$	parameter indicating lag time
$k_D$	a constant related to the depression storage capacity
$k_f$	decay constant in infiltration equation $k$
$k_I$	a constant related to depression storage capacity
$l$	length parameter
$l_i$	length of travel from the center of an impervious area to the outflow point of a watershed
$n$	Manning's roughness coefficient
$p_e$	rate of rainfall excess
$q$	rate of outflow
$q_{max}$	maximum peak rate of outflow
$t$	time parameter
$t_e$	watershed characteristic time
$t_m$	storage delay time
$t_R$	rise time of the unit hydrograph
$x$	length parameter
$y$	depth parameter
$\bar{y}$	mean depth of flow
$\alpha$	coefficient of runoff
$\theta_o$	soil moisture index
$\tau$	scaled time parameter
$\tau_L$	travel time in the characteristic reach
$\phi$	degree of channelization
$\sigma_c$	capacity rate of inflow into surface depression storage
$\sigma_a$	actual rate of inflow into surface depression storage

in which

$$\begin{aligned} q_{\max} &= i(1 - e^{-1/k}) \\ k &= \text{parameter indicating lag time} \\ \tau &= t - 1 \end{aligned}$$

### 3. Synthesis of the total runoff hydrograph by the unit hydrograph method.

James (1965) studied the effects of urban development on flood peaks using a digital computer based on the Stanford watershed model. The object of his study was to develop a long-term continuous hydrograph for Morrison Creek, Sacramento County, California. By varying constants which describe the physical conditions within the watershed according to the amount of urban development and channel improvement within the tributary area, a number of continuous hydrographs were developed. In this way flood peaks were estimated for various combinations of percentage impervious area, degree of channelization, and number of tributary areas.

In the study by James (1965), the watershed condition was separated for analysis into urbanization and channelization. Urbanization was defined to include all factors affecting runoff other than the cross section or the alignment of the channels. Channelization was defined to account for the hydrologic effects of changes in channel geometry and alignment from the natural state to a larger and straighter prismatic form. This distinction between urbanization and channelization was made in order to allow for the use of zoning and channel improvement in flood control planning.

James attempted to relate the independent variables (urbanization, channelization, and tributary area) with the dependent (but observed) flood peaks. In his models, the following inputs were altered to represent changes in the degree of urbanization. They are:

1. Advance of the time-area histogram of inflows to reflect the probable installation of storm sewers.
2. Increase in the impervious area.
3. Decrease in maximum hourly interception and depression storages because of the reduction in undrained natural depressions with increase in urbanization.
4. Reduction in upper zone soil moisture storage.
5. Reduction in overland flow delay.
6. Reduction in interflow delay.

James concluded from his study that impervious cover and channelization are the most important parameters of urbanization that significantly affect the runoff process in the urban watershed.

Espey, Jr., et al (1965) made a similar study on the evaluation of urbanization effects on the runoff characteristics of urban watersheds located in the region of Austin, Texas. Empirical equations were developed by linear multiple regression analysis to determine rural and future urban unit hydrographs and to evaluate the effects of both existing and future urbanization on the runoff characteristics. Except for the time of rise, each regression equation utilized the drainage area as the most dominant parameter. For determining the 30-minute unit hydrograph for rural watersheds, the following equations were developed from the data of 11 rural watersheds in Texas, Oklahoma, and New Mexico.

$$T_{RR} = 2.65 L^{0.12} S^{-0.52} \dots \dots \dots (1.25)$$

$$Q_R = 1.70 \times 10^3 A^{0.88} T_R^{-0.30} \dots \dots \dots (1.26)$$

$$T_{BR} = 7.41 \times 10^3 A^{0.64} Q^{-0.53} \dots \dots \dots (1.27)$$

$$W_{50R} = 7.37 \times 10^4 A^{1.11} Q^{-1.13} \dots \dots \dots (1.28)$$

$$W_{75R} = 4.46 \times 10^4 A^{1.06} Q^{-1.13} \dots \dots \dots (1.29)$$

The expressions, for the 30-minute unit hydrograph for urban watersheds, based on data from 22 watersheds throughout the United States, are given below:

$$T_{RU} = 20.8 \phi L^{0.29} S^{-0.11} T^{-0.61} \dots \dots \dots (1.30)$$

$$Q_U = 1.93 \times 10^4 A^{0.91} T_{RU}^{-0.94} \dots \dots \dots (1.31)$$

$$T_{BU} = 4.44 \times 10^5 A^{1.17} Q^{-1.19} \dots \dots \dots (1.32)$$

$$W_{50U} = 4.14 \times 10^4 A^{1.03} Q^{-1.04} \dots \dots \dots (1.33)$$

$$W_{75U} = 1.34 \times 10^4 A^{0.94} Q^{-0.94} \dots \dots \dots (1.34)$$

in which

$T_R$  = time of rise of the unit hydrograph

$I$  = percentage impervious cover

$Q$  = peak discharge

$T_B$  = time base

$\phi$  = urban factor

$W_{50}, W_{75}$  = hydrograph widths at 50 and 75 percents of the peak discharge respectively.

Subscript U (as in  $T_{BU}$  or  $T_{RU}$ ) represents the urban watershed

Subscript R (as in  $Q_R$  or  $T_{RR}$ ) represents the rural watersheds

Because no data were obtained before urbanization and only nine years of record were available for the Waller Creek watershed, the above derived rural and urban equations were used by Espey, Jr., et al. to evaluate the effects of urbanization on the hydrologic characteristics of the Waller Creek watershed. Comparison of the measured and rural unit hydrographs indicated that the peak discharge has been increased by only 6 percent while the time of rise has been reduced by 47 percent due to present conditions of urbanization. The authors felt that additional ur-



banization data were needed to develop more reliable and general relationships applicable to both urban and rural watersheds.

According to Schaake, Jr., (1965) the greatest problem in synthesizing the runoff hydrograph in urban areas is one of accounting properly for the distribution of the water among the various phases of the runoff process. He assumed that, for paved areas, the rate at which water enters depression storage would be neglected. To describe the flow occurring in the various parts of a drainage area during a storm, the drainage was divided into a number of components. For example, a parking lot would drain to a swale, with the swale draining to a storm water inlet. The equations for gradually varied unsteady flow in open channels were then used to describe the flow in each of the component parts of the larger areas. This was applied only to paved areas.

The urban hydrology research, reviewed thus far, has dealt with the evaluation of the effects of urbanization on the runoff hydrograph characteristics, such as the lag time and the peak discharge. Detailed mathematical modeling was limited to small impervious areas. Large urban watershed studies were mainly statistical. Since an urban watershed is comprised of both impervious and pervious areas intermingled in a complex manner, the quantitative modeling of such a system is relatively a difficult proposition. The problem is one of determining the rainfall excess from urban areas with varying surficial characteristics of roughness and abstraction, and properly routing this excess through overland and channel storages.

### Analog computer application

Recent advances in computer technology have widened the horizon for hydrologists and engineers in search of appropriate methodologies for simulation of the physical problems. Techniques, which until recently were untapped because of the laborious computations involved, are now being pursued with great interest. Two complex methods of hydrograph synthesis that required the use of a digital computer have been developed; one by Crawford and Linsley (1962) and the other by Dawdy and O'Donnell (1965).

The electronic analog computer is one of the modern computer tools which gained wide usage during the World War II and is now found to be almost as useful as the digital computer. The types of problems best adapted to solution on an electronic analog computer are those involving systems of simultaneous differential equations (linear or nonlinear). Another important area, where the

electronic analog computers are found to be increasingly useful, is simulation. Simulation is a technique in which the behavior or response of a dynamic system to given inputs and constraints is studied. Shen (1965) envisioned the use of the analog computer for analyzing the flood runoff. Harder, et al. (1966) and Otoba, et al. (1965) successfully applied analog simulation techniques for analyzing flood flows in rivers.

Research in the development of electronic analog models of dynamic flow systems began at Utah State University in 1963. Early emphasis was placed on designing and building an electronic analog computer whose capabilities in terms of hydrologic definition and the computer capacity were not high. The primary objective of the earliest model was to demonstrate the feasibility of modeling the physical processes involved in the hydrologic system (Bagley, et al. 1963). This first analog computer model was found to be satisfactory for the study of interbasin effects and other hydrologic problems where simulation of hydrologic process in detail was not required. Encouraged by the success of this early model, Riley, et al. (1966, 1967) proceeded to develop more versatile analog models which included improvement of relations for describing various hydrologic processes. At the same time the analog computer has also been improved with respect of its flexibility and capability for the solution of the hydrologic problems.

The analog computer is considered valuable in solving problems where the physical behavior of the system is analogous to that of the electronic system. Since all the computations proceed simultaneously, the computation time is not significantly altered if the size of the problem is increased. Increasing the problem size may, however, require more analog hardware.

The only available independent variable on an analog computer is time, and computations are performed continuously throughout the integration period. Considering that most of the hydrological processes which occur in nature are time dependent and therefore differential in form, they are easily handled by the analog computer. In general, it is necessary to input the data to the analog computer in its digital format. This can be easily accomplished when the period of integration coincides with the finite period of the recorded data. Riley, et al. (1967) concluded that the problem of representing the individual hydrologic processes and of synthesizing them into a complex system can be adequately accomplished with an electronic analog computer. The exactness and the utility of such a model are dependent upon the quantity and reliability of the data representing the variable watershed characteristics, storm patterns, and channel routing.

## CHAPTER II DEVELOPMENT OF THE PHYSICAL MODEL

The abstractive processes, such as interception, infiltration, and depression storages on any urban watershed occur in the same way as those on natural or rural watersheds. The problem is one of accounting for these losses from the heterogeneous conglomeration of pervious and impervious areas. Each component area contributes differently to the runoff process between the occurrence of rain and the time when it becomes runoff at any point of measurement. A correct hydrograph of rainfall excess and an adequate routing procedure through the drainage system for transforming the rainfall excess to the runoff at a specified point on the watershed are essential parts of any adequate mathematical model.

### Modeling Procedure

In the development of an urban watershed model under this study, the following steps were adopted as a logical procedure:

1. Identification and definition of measurable urban parameters.
2. Mathematical description of the various phases of the runoff process in terms of the physical characteristics of the watershed (watershed coefficients).
3. Verification of the mathematical model on an analog computer by simulation of several recorded runoff events.
4. Determination of the watershed coefficients from model verification and relating them to the corresponding urban parameters.
5. Prediction of future urban parameters and determination of the corresponding watershed coefficients.

To use the model, thus developed, for prediction purposes, information on the following parameters would be needed.

1. Estimates or exact values of the urban parameters in the year for which the stream flow is to be predicted.
2. Estimated or assumed design storm hyetographs.

The functional or graphical relationships developed between the urban parameters and the watershed coefficients (step 4) could be used to determine the values of the watershed coefficients corresponding to the estimated urban parameters. By utilizing these values of the watershed coefficients and the appropriate design storm hyetograph as input into the model, the outflow hydrograph could be predicted.

### Urban Parameters

The characteristics of urbanization considered in the present study are (1) the percentage impervious cover, and (2) the characteristic impervious length factor.

The percentage impervious cover,  $C_f$ , is defined as the ratio of the total impervious area (area covered by houses, roads, and parking areas) to the total watershed area. This factor is an index that characterizes the various abstractive processes which materially alter the time distribution and total volume of rainfall excess.

The characteristic impervious length for a particular impervious element (area  $a_i$ ) of a watershed is defined as the length of travel,  $l_i$ , between the center of the area and the discharge measuring point (Figure 2.1).

The mean characteristic impervious length,  $L_m$ , for the watershed is given by

$$L_m = \frac{\sum a_i l_i}{\sum a_i} \dots \dots \dots (2.1)$$

where  
 $l_i$  = length of travel from the center of the  $i^{\text{th}}$  impervious element  
 $a_i$  = area of the  $i^{\text{th}}$  impervious element

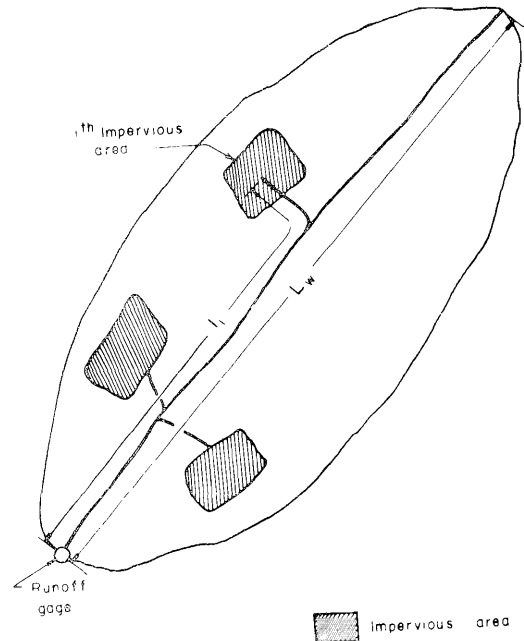


Figure 2.1. Schematic sketch illustrating characteristic impervious length.



### CHAPTER III

#### DESCRIPTION OF THE EXPERIMENTAL WATERSHED

The model, developed for evaluating the various effects of urbanization on the runoff characteristics of small watersheds, is tested and verified with data from Waller Creek watershed located within the metropolitan area of Austin, Texas (Figure 3.1). Selection of this watershed was influenced by the fact that good data were available and some useful work had already been completed by the Center for Research in Water Resources of the University of Texas (Espey, Jr., et al., 1965). The U.S. Geological Survey has compiled and made available rainfall and runoff data from this watershed since 1954. In addition, the U.S. Department of Agriculture (USDA) Agriculture Research Service has aerial photos for this watershed from flights made in the years 1951, 1958, and 1964. A summary of the description of climate, geology, topography, instrumentation and drainage conditions of the study area reported by Espey, Jr., et al. (1965) is presented in the following paragraphs.

Waller Creek is a tributary of the Colorado River of Texas which drains to the Gulf of Mexico. The drainage area of this watershed is 4.13 square miles and lies above 23rd Street (Figure 3.2). Within this area there is a less urbanized subwatershed of 2.31 square miles above 38th Street.

#### Climate

The climate of this region is mild and semi-humid. The weather during the March through October period is warm. The mean annual precipitation is about 33.5 inches with a fairly uniform distribution of precipitation throughout the year. Heavy intensities of precipitation are not uncommon particularly from tropical or semi-tropical storms.

#### Geology

Geologically, this watershed is located in the west gulf coastal plain and is underlain by two bedrock formations and a thin alluvial formation. Eagle Ford Shale underlies the extreme northwestern part of the watershed. The remaining area is underlain by Austin Chalk. The Austin Chalk weathers to a heavy black clay soil of a low permeability. The bedrock formations are covered in the southern part by an alluvial terrace of the ancient Colorado River.

#### Topography

The area consists of gently rolling, hilly land and is characterized by glaring outcrops of limestone on the slopes and in the bluffs of the creek. The maximum width

of this long and narrow area is 2.6 miles at 45th Street and the minimum width is 0.9 miles near the gaging station. The average slope,  $S$ , of the main channel is 0.009 ft./ft. and is fairly uniform (Diehl, 1959). The mean basin slope,  $S$ , (Eagleson, 1962) as shown by Table 3.1 is approximately the same as the average slope,  $S$ .

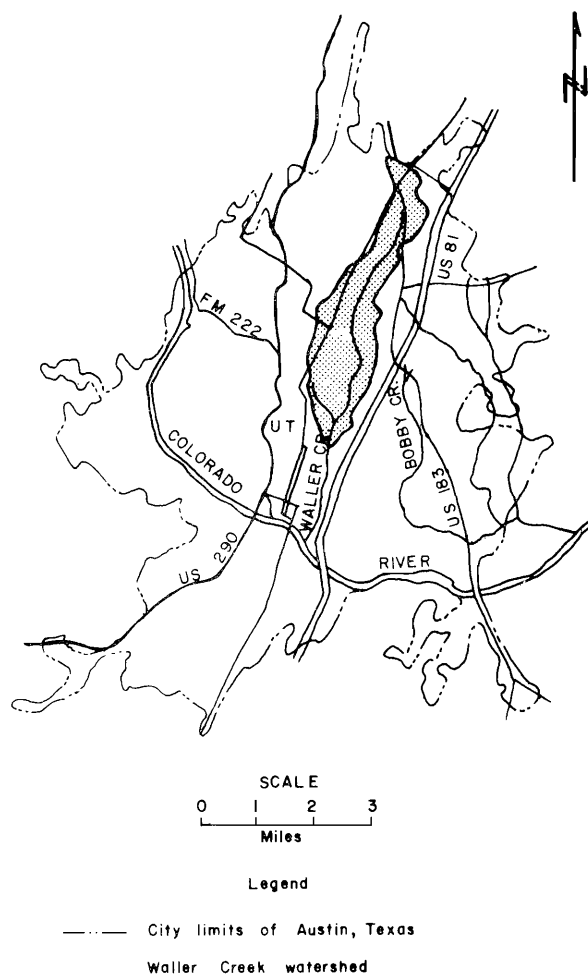


Figure 3.1. Map of Austin, Texas showing location of Waller Creek watershed.

Table 3.1. Geometric particulars of Waller Creek watershed.

Station	$\bar{S}$ (ft/ft)	$\bar{H}$ (ft)	$\bar{L}$ (ft)	$L_{ca}$ (ft)	$S=H/L$ (ft/ft)	$A$ (miles <sup>2</sup> )	$L$ (ft)
23rd Street	.0124	134	10,800	10,500	.009	4.13	27,600
38th Street	.0126	125	9,940	13,000	.009	2.31	23,080

### Instrumentation

There are five rain gages (two non-recording and three recording) and two stream flow stations on this watershed. The location of these gages is shown in Figure 3.2. The two stream flow stations are equipped with standard A-10 Stevens recorders.

### Drainage Conditions

The head waters of Waller Creek are located south of Anderson Lane, in the northern part of the city. The main channel has been extended by excavation to the natural divide just north of Croslin Street (Figure 3.2). A drainage ditch joins the main channel just south of where it crosses Airport Boulevard. The drainage ditch was formed by the Texas and New Orleans Railroad track and this was reported to contribute additional runoff from an area of 0.3 square miles.

A second branch, called West Branch, originating in the general area of west 45th Street and Lamar, joins the main channel just west of San Jacinto Boulevard approximately two blocks above the 23rd Street stream gaging station. Beginning in the Hemphill Park area this second branch is a rock-lined channel varying in cross section from trapezoidal to rectangular in shape between 32nd Street and just south of west 30th Street where the rock lining ends.

Based on field observations and studies of aerial photographs, it is estimated that approximately one-third of the basin is undeveloped, with the remaining two-thirds classified as new business and old and new residential (Diehl, 1959). Many small diversions caused by storm sewers and embankments are present within the natural basin.

### Urban Parameters

As extensive study of the watershed has been completed using aerial photographs made in 1951, 1958, and 1964. Photo enlargements, 1 in. = 275 ft., were obtained from the 1964 flight.

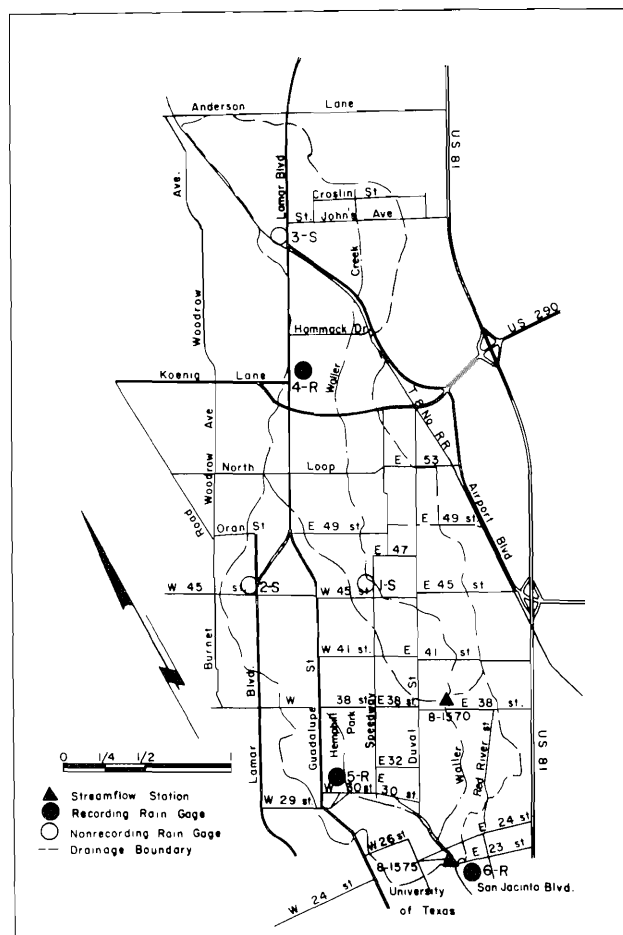


Figure 3.2. Instrumentation of Waller Creek watershed.

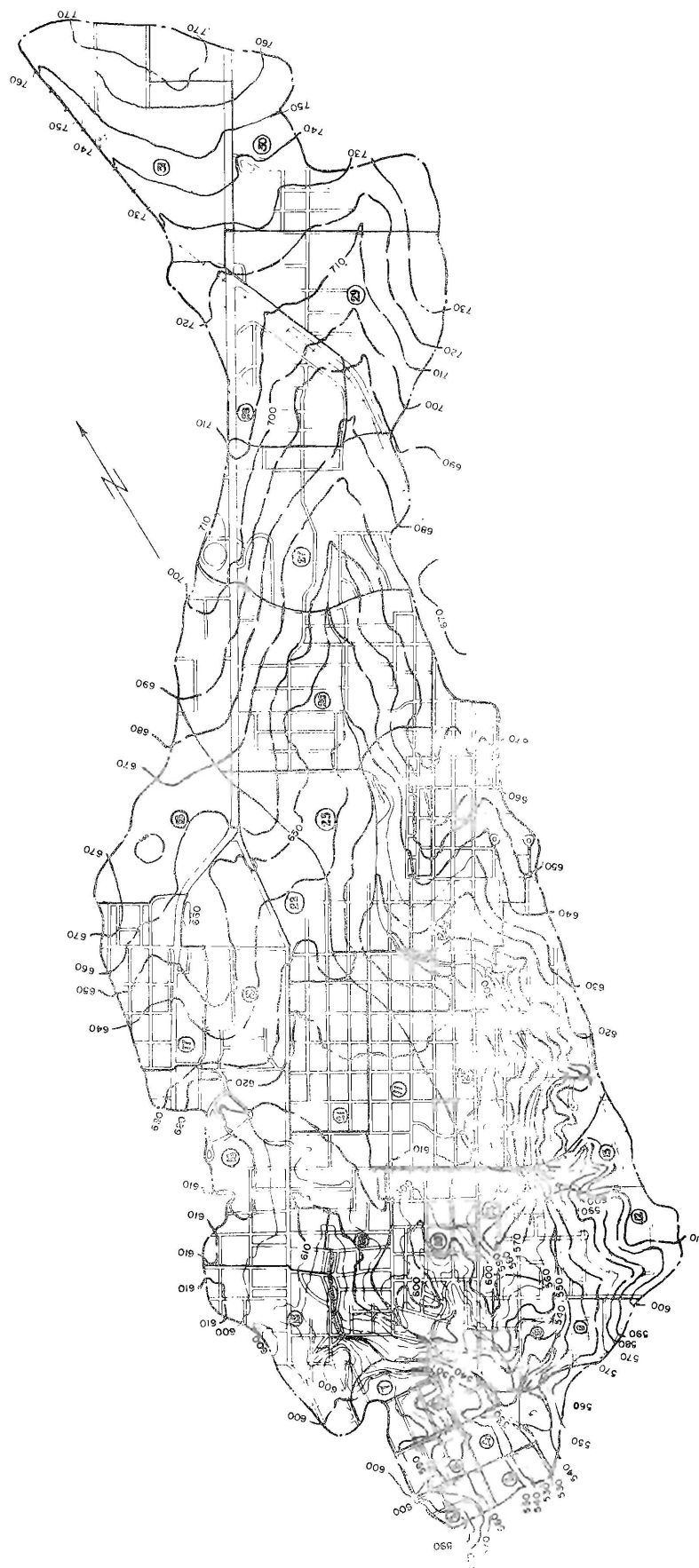


Figure 3.3. Water Creek watershed with subunits.

## Percentage impervious cover

The aerial photographs were optically enlarged to a scale of 1 in. = 500 ft. and the impervious areas were transferred to a base map of the same scale. The watershed was subdivided into subunits (Figure 3.3) and the impervious areas in each of the subunits were computed. Typical subunits, for each of the three years, are shown by Figures 3.4, 3.5, and 3.6. Table 3.2 gives details of the impervious areas in each of the subunits.

The variation of percentage impervious cover,  $C_f$ , with reference to time is shown by Figure 3.7.  $C_f$  is found to vary linearly with time. The value of  $C_f$  for 38th Street watershed is initially less than that of the 23rd Street, but the extrapolated values of  $C_f$  in the year 1967 for both watersheds are equal. This suggests that the extent of urbanization in both watersheds in 1967 is approximately of the same proportion.

From Figure 3.7 the following expressions for  $C_f$  were derived for both watersheds:

$$\begin{aligned} \text{23rd Street } C_f &= .265 + .0082 t \\ \text{38th Street } C_f &= .225 + .0102 t \end{aligned} \quad \text{for } t < 21$$

where

$$t = \text{number of years since 1950}$$

These expressions are adopted to interpolate the values of  $C_f$  for the years from 1950 to 1970 for use in the computations elsewhere. Some revision in these expressions might be necessary for later years on the basis of aerial photographs from subsequent flights.

## Characteristic impervious length factor

The average length from the center of the impervious cover in each of the subunits to the outflow gaging points (Figure 2.1) were measured from the base map using a rotometer. Table 3.3 gives the computed values of these characteristic impervious lengths,  $\ell_i$ , for each of the subunits in various years.

The mean characteristic length of the impervious cover for the watershed,  $L_m$ , is computed using the following expression:

$$L_m = \frac{\sum_{i=1}^n a_i \ell_i}{\sum_{i=1}^n a_i} \quad \dots \dots (3.1)$$

where

- $a_i$  = area of impervious cover in  $i^{\text{th}}$  subunit of the watershed
- $\ell_i$  = length from the center of the impervious cover in  $i^{\text{th}}$  subunit to the runoff gaging point

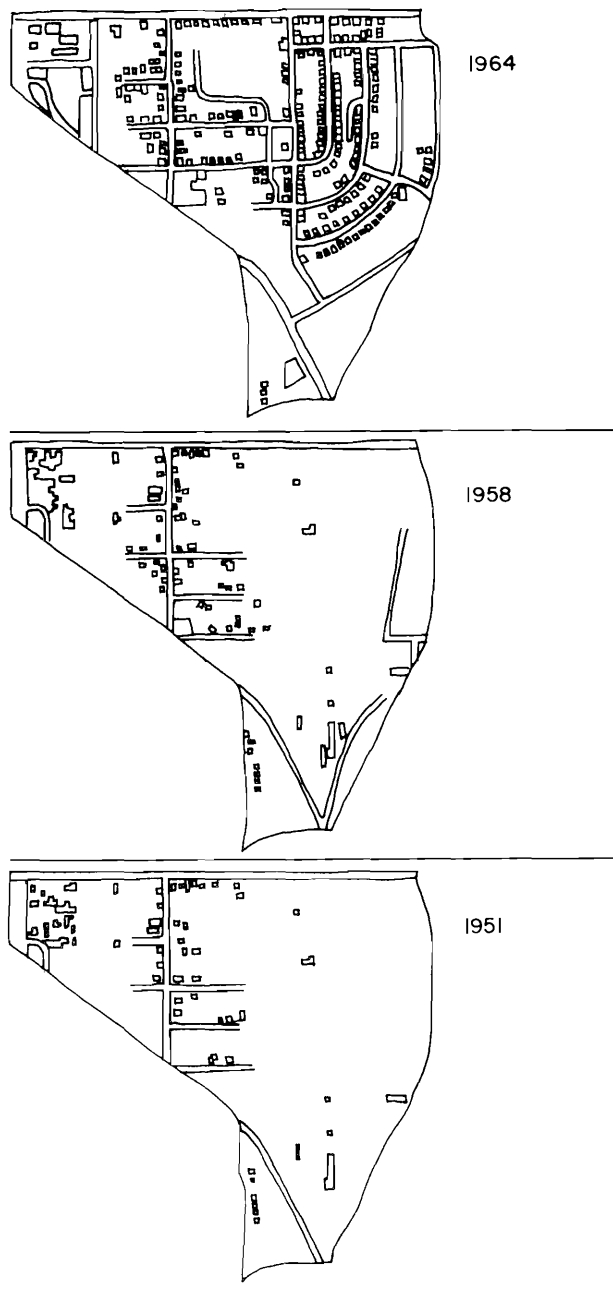


Figure 3.4. Urbanization in subunit 29 during the years 1951, 1958, and 1964.

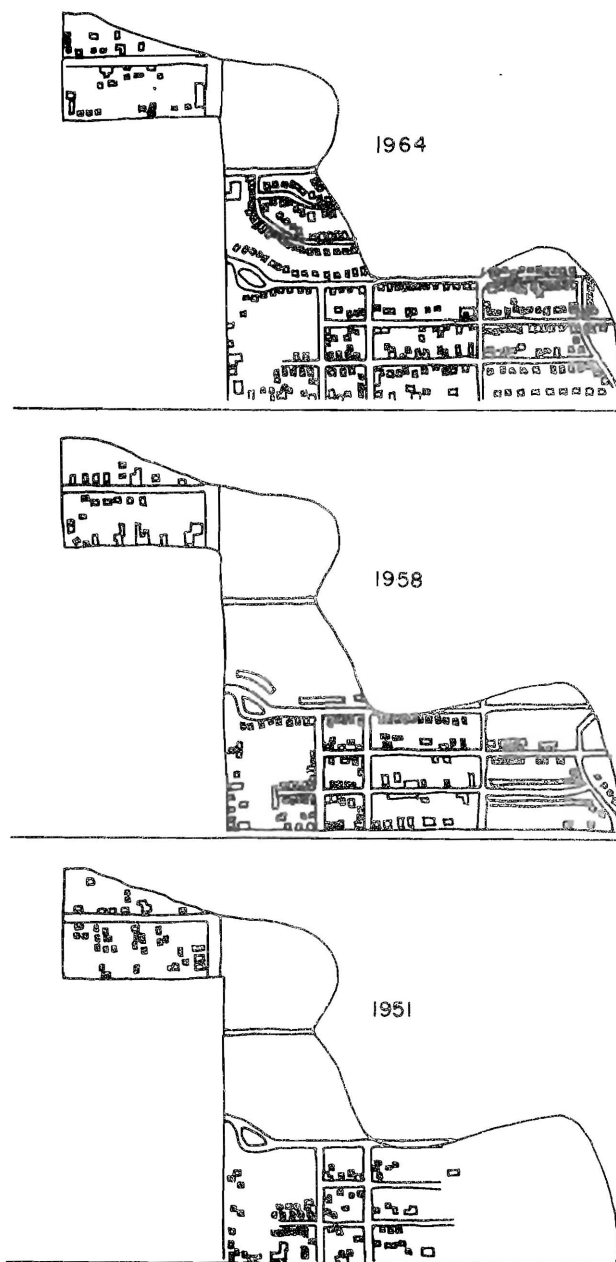


Figure 3.5. Urbanization in subunit 30 during the years 1951, 1958, and 1964.

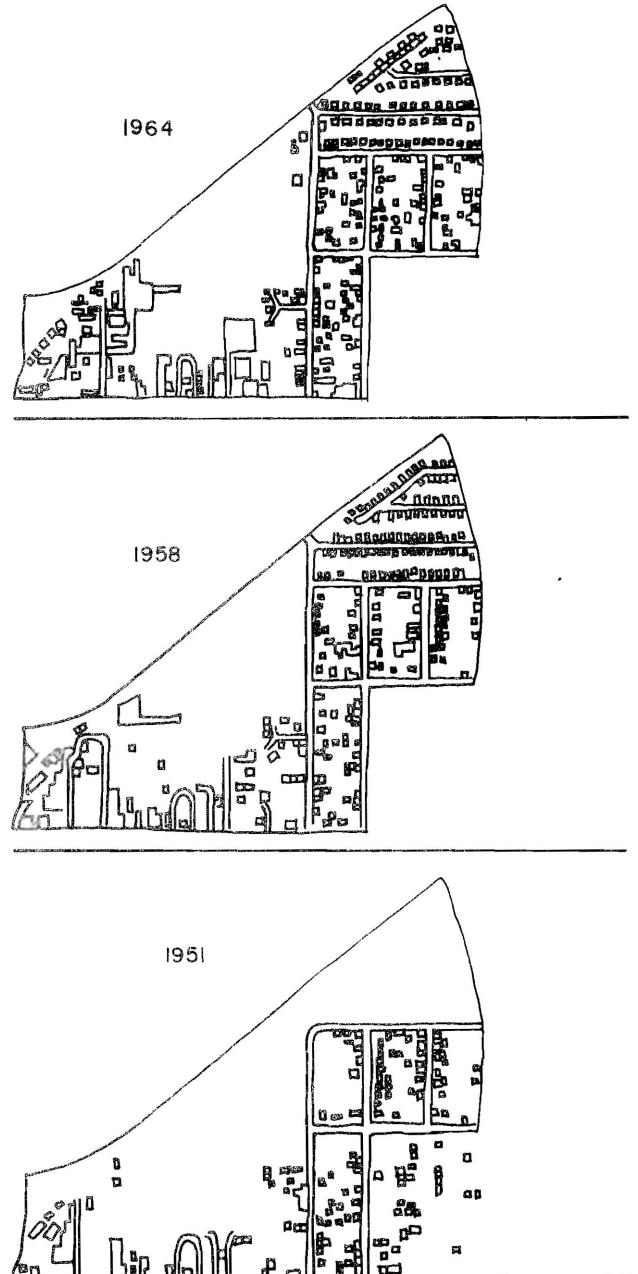


Figure 3.6. Urbanization in subunit 31 during the years 1951, 1958, and 1964.



Table 3.2. Impervious areas in the subunits.

Subunit No.	Total area of subunit	Impervious Areas		
		Years		
		1951	1958	1964
1	261	99	99	99
2	233	187	187	187
3	345	162	162	162
4	219	31	31	31
5	366	55	55	55
6	499	154	154	154
7	260	56	56	56
8	440	122	122	122
9	584	152	152	152
10	1745	646	646	646
11	989	345	345	345
12	875	321	321	321
13	524	117	117	117
14	945	369	369	369
15	1022	555	659	672
16	1662	535	658	678
17	1350	420	546	609
18	1388	126	300	300
19	2084	439	492	600
20	1455	532	649	723
21	1180	571	574	574
22	922	140	176	206
23	3121	639	973	1117
24	2839	1123	1235	1340
25	2403	548	548	548
26	3962	1299	1677	1834
27	2798	518	762	1120
28	1499	610	708	804
29	2631	307	341	946
30	2111	291	506	686
31	<u>2652</u>	<u>335</u>	<u>770</u>	<u>806</u>
Total for				
23rd Street	43364	11804	14390	16379
Percentage				
for 23rd Street		.272	.332	.378
Total for				
38th Street	24016	5670	7520	9191
(sum of areas of				
subunits from 23rd subunit)				
Percentage for 38th Street				
		.236	.313	.364

(Note: 100 units of the areas in the table is equal to 6.25 acres of actual area)

Table 3.3. Characteristic impervious lengths ( $l_i$ ).

Subunit No.	Years					
	38th Street			23rd Street		
	1951	1958	1964	1951	1958	1964
	ft. in.	ft. in.	ft. in.	ft. in.	ft. in.	ft. in.
1				$0-4\frac{11}{16}$	$0-4\frac{11}{16}$	$0-4\frac{11}{16}$
2				$0-2\frac{6}{8}$	$0-2\frac{6}{8}$	$0-2\frac{6}{8}$
3				$0-4\frac{5}{6}$	$0-4\frac{5}{6}$	$0-4\frac{5}{6}$
4				$0-2\frac{13}{24}$	$0-2\frac{13}{24}$	$0-2\frac{13}{24}$
5				$0-3\frac{15}{16}$	$0-3\frac{15}{16}$	$0-3\frac{15}{16}$
6				$0-6\frac{1}{3}$	$0-6\frac{1}{3}$	$0-6\frac{1}{3}$
7				$0-6\frac{1}{2}$	$0-6\frac{1}{2}$	$0-6\frac{1}{2}$
8				$0-6\frac{19}{24}$	$0-6\frac{19}{24}$	$0-6\frac{19}{24}$
9				$0-5\frac{23}{48}$	$0-5\frac{23}{48}$	$0-5\frac{23}{48}$
10				$0-8\frac{5}{24}$	$0-8\frac{5}{24}$	$0-8\frac{5}{24}$
11				$1-0\frac{17}{32}$	$1-0\frac{17}{32}$	$1-0\frac{17}{32}$
12				$0-9\frac{11}{12}$	$0-9\frac{11}{12}$	$0-9\frac{11}{12}$
13				$1-1\frac{5}{16}$	$1-1\frac{5}{16}$	$1-1\frac{5}{16}$
14				$0-10\frac{5}{16}$	$0-10\frac{5}{16}$	$0-10\frac{5}{16}$
15				$0-11\frac{5}{6}$	$1-0\frac{5}{24}$	$1-0\frac{5}{24}$
16				$1-2\frac{25}{64}$	$1-3\frac{15}{24}$	$1-3\frac{15}{24}$

Subunit No.	Years					
	38th Street			23rd Street		
	1951	1958	1964	1951	1958	1964
	ft. in.	ft. in.	ft. in.	ft. in.	ft. in.	ft. in.
17				$1-7\frac{3}{4}$	$1-10\frac{20}{24}$	$1-10\frac{20}{24}$
18				$2-2\frac{15}{24}$	$2-3\frac{11}{32}$	$2-3\frac{11}{32}$
19				$1-8\frac{3}{8}$	$1-7\frac{33}{40}$	$1-7\frac{33}{40}$
20				$1-1\frac{7}{8}$	$1-1\frac{26}{40}$	$1-1\frac{26}{40}$
21				$1-3\frac{7}{8}$	$1-6\frac{4}{24}$	$1-6\frac{4}{24}$
22				$1-9\frac{3}{4}$	$1-10\frac{1}{8}$	$1-10\frac{1}{8}$
23	$0-6\frac{25}{32}$	$0-7\frac{47}{48}$	$0-7\frac{47}{48}$	$1-5\frac{9}{32}$	$1-6\frac{23}{48}$	$1-6\frac{23}{48}$
24	$0-11\frac{3}{8}$	$0-11\frac{51}{56}$	$0-11\frac{51}{56}$	$1-9\frac{7}{8}$	$1-10\frac{23}{56}$	$1-10\frac{23}{56}$
25	$1-0\frac{1}{12}$	$1-1\frac{1}{32}$	$1-1\frac{1}{32}$	$1-10\frac{7}{12}$	$1-11\frac{17}{32}$	$1-11\frac{17}{32}$
26	$1-7\frac{6}{8}$	$1-9\frac{39}{96}$	$1-9\frac{39}{96}$	$2-6\frac{1}{4}$	$2-7\frac{39}{96}$	$2-7\frac{39}{96}$
27	$1-11\frac{13}{28}$	$1-11\frac{7}{8}$	$1-9\frac{22}{24}$	$2-9\frac{27}{28}$	$2-10\frac{3}{8}$	$2-8\frac{10}{24}$
28	$2-5\frac{5}{6}$	$2-6\frac{3}{10}$	$2-6\frac{1}{24}$	$3-4\frac{1}{3}$	$3-4\frac{8}{10}$	$3-4\frac{13}{24}$
29	$2-8\frac{7}{16}$	$2-8\frac{1}{6}$	$2-9\frac{1}{4}$	$3-6\frac{15}{16}$	$3-6\frac{4}{6}$	$3-7\frac{3}{4}$
30	$3-1$	$2-11\frac{29}{40}$	$3-1\frac{22}{24}$	$3-11\frac{1}{2}$	$3-10\frac{9}{40}$	$4-0\frac{10}{24}$
31	$3-3\frac{27}{40}$	$3-3\frac{46}{48}$	$3-4\frac{13}{48}$	$4-1\frac{27}{40}$	$4-2\frac{22}{48}$	$4-2\frac{37}{48}$

(Note: 1 inch of the length unit in the table is equal to 500 ft. of actual length.)

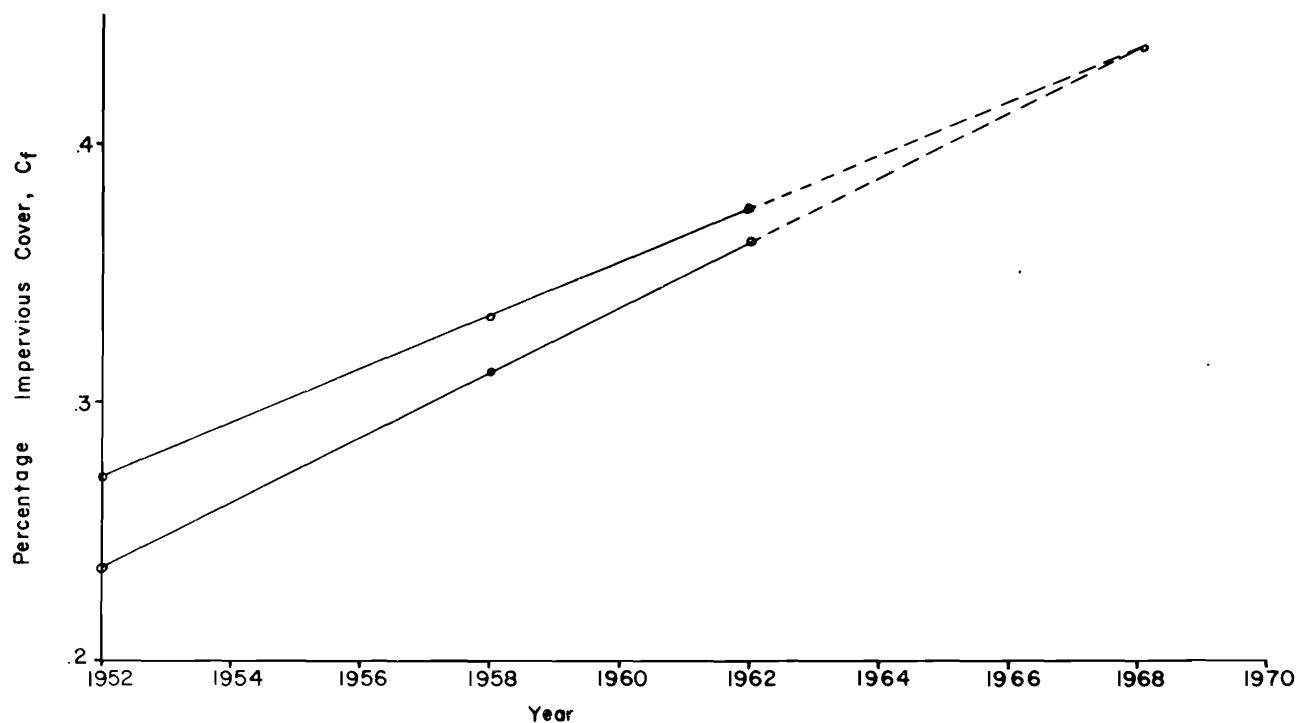


Figure 3.7. Yearly variation of percentage impervious cover.

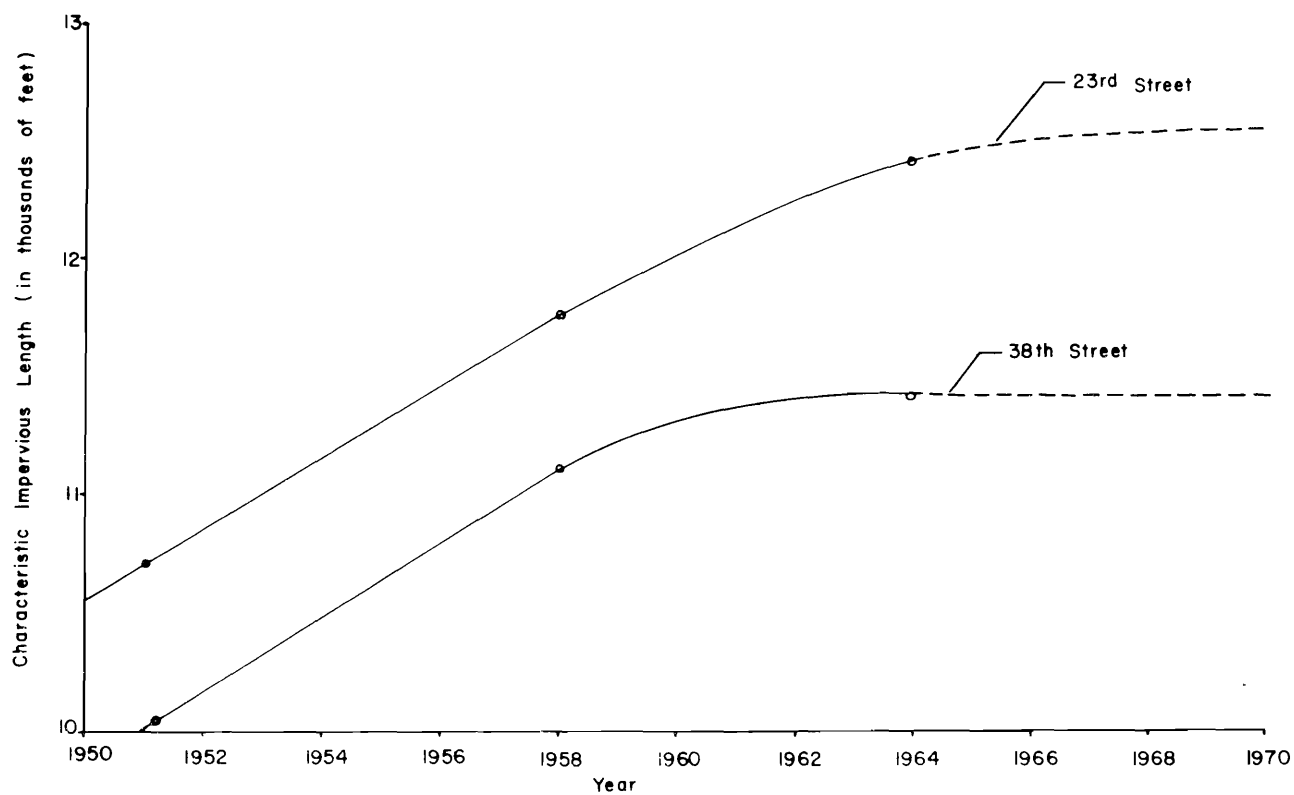


Figure 3.8. Yearly variation of mean characteristic impervious length.

The characteristic impervious length factor,  $L_f$ , is then obtained from the expression

$$L_f = \frac{L_m}{L} \quad \dots \dots \dots (3.2)$$

where

$L$  = maximum length of travel on the watershed (Figure 2.1)

Table 3.4 summarizes the chronological development of the urban parameters of the 23rd and 38th Streets watersheds within the Waller Creek basin. The relation between the mean characteristic impervious length,  $L_m$  and time is shown by Figure 3.8. The value of  $L_m$  for both watersheds initially increases relatively rapidly up to the year 1958. From 1958 onward, the rate of increase of  $L_m$  with re-

spect to time is slow. This observation, when considered in conjunction with the variation in  $C_f$ , indicates that while the impervious cover,  $C_f$ , is increasing, the relative location of new impervious areas with respect to the runoff measuring point is not significant enough to change the mean characteristic impervious length  $L_m$  in the watershed. In other words, urbanization is proceeding in such a way that its effect on the time distribution of runoff is mainly due to the changes in the impervious cover as represented by  $C_f$ .

Beyond the year 1964, the values of  $L_m$  in both the watersheds are expected to remain at constant values (Figure 3.8). It is also expected that the percentage impervious cover on the watershed will not exceed 0.5 to 0.6. The values of  $L_m$  for use in the computation elsewhere are obtained from Figure 3.8.

**Table 3.4. Chronological development of urbanization.**

	Total Area	Percentage Impervious Area ( $C_f$ )			Actual Mean Characteristics Impervious Lengths ( $L_m$ )		
		Sq. Miles			ft.	ft.	ft.
		1951	1958	1964	1951	1958	1964
23rd Street	4.13	.272	.332	.378	10,727	11,753	12,409
38th Street	2.31	.236	.313	.364	10,031	11,120	11,406



## CHAPTER IV ANALOG COMPUTER PROGRAMMING

The behavior of the system under study, or the problem to be solved, is first expressed by a set of algebraic or differential equations. The mathematical model adopted for this study is described in Chapter II. Complex mathematical models of this type can be synthesized and solved by use of high speed computers. For the study discussed herein, the model is programmed and solved on an analog computer.

The analog computer consists of an assemblage of computing units or elements, each capable of performing some specific mathematical operation, such as addition, multiplication, or integration, and these units are interconnected so as to generate solutions to the problem. There are two dependent variables in electrical circuits. They are (1) the voltages across the circuit elements or from node points to ground and (2) the currents through each element. Voltages are used almost exclusively as the computing variable in electric analogs because these can be measured and recorded at any point in the electrical circuit by a voltmeter attached in parallel with the circuit element and without any circuit modification. On the other hand, to measure the current through an element, it is necessary to open the circuit and to introduce an ammeter in series with the element.

In electronic analog computers, time is necessarily the independent variable. All the dependent variables must therefore be functions of the independent variable time, so that their derivatives are with respect to time.

The programming of a physical problem makes use of this characteristic time dependent behavior of the analog variables, so that the dependent and independent physical variables are represented with suitable scale(s) in terms of the dependent analog variable, voltage, and the independent analog variable, time.

An electronic analog computer is employed to solve the physical problem of runoff simulation represented by the schematic model (Figure 1.1). The problem consists of the representation of the mathematics involved in the following physical phenomena by analog computing units.

1. Precipitation
2. Interception
3. Infiltration
4. Depression storage
5. Routing of rainfall excess

Precipitation is the input to the model. The phenomena of interception, infiltration, and depression storage represent the losses to be deducted from the input in compatible time units. The surplus of precipitation remaining after the demands of the various losses have been met is termed the rainfall excess. In the final stages, the rainfall excess is routed through the transient effects of overland and channel storages to yield the outflow hydrograph. In terms of the analog computer representation, these phenomena are shown by Figure 4.1. The details of this representation are discussed in the following sections.

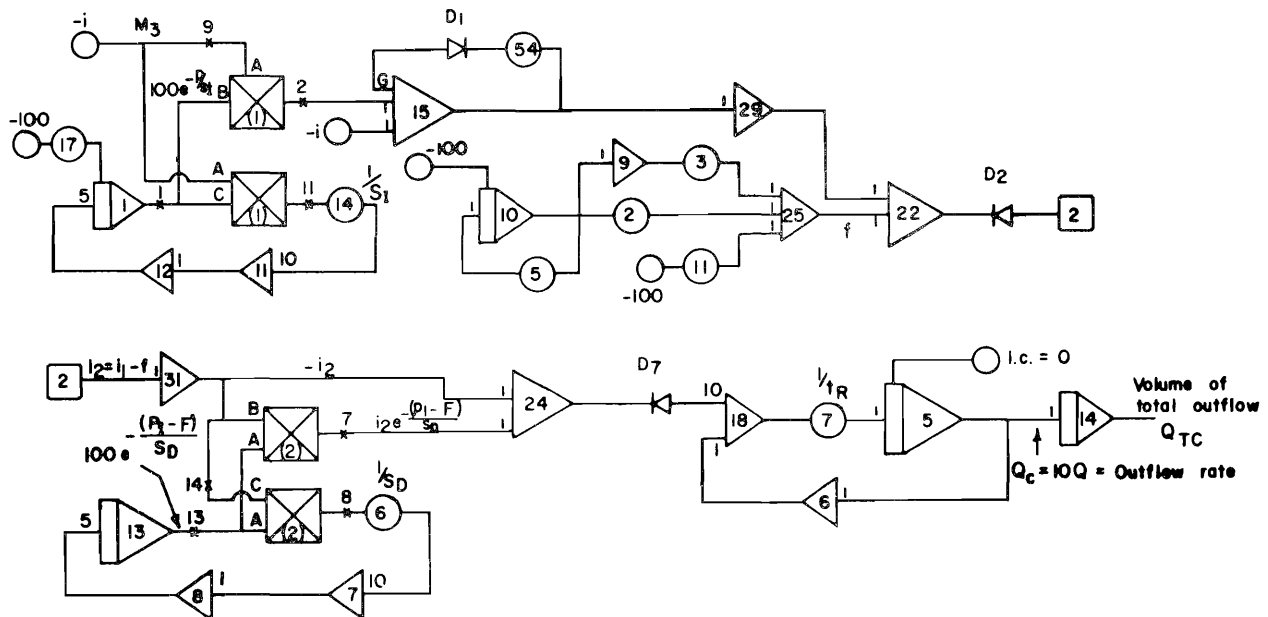


Figure 4.1. Analog computer program for outflow hydrograph from equivalent rural watershed.

## Precipitation

The precipitation occurring in any particular storm, for which the outflow hydrograph is to be synthesized, is the input to the model. Since voltage is the most convenient dependent variable available on the analog computer, the precipitation is applied to the analog model in the form of voltage either as a continuous function or as a staircase step function.

The analog computer equipment at Utah Water Research Laboratory, Utah State University, Logan, Utah has facilities for applying the inputs in both forms. Continuous hyetographs of precipitation can be generated by the use of either diode function generators or scanning photoformers. This procedure is advantageous when the rainfall records are available in the form of continuous functions.

The precipitation data, obtained from the U.S. Geological Survey office in Austin, Texas, are in the digital form. In such cases, the input is conveniently applied in the form of a step function. The input device, adopted in this study consists of servo-driven potentiometric function generators. The automatic relay mechanism switches the mechanical wipers from one potentiometer to the other in one second. In order to use this type of equipment, the precipitation data should be available in equal time intervals of the storm. The precipitation data from the U.S. Geological Survey, recorded in unequal time intervals, is therefore converted to equal time interval values by a separate digital program (Appendix A).

There are 12 potentiometers (steps) available on the input device and so most of the storms analyzed are divided into 12 equal intervals of time. The values of precipitation occurring in each of these time intervals are converted to voltage by appropriate scaling. The high end of each of these potentiometers are connected to  $\pm 100$  volts depending upon the sign of input needed in the main program. Each of the potentiometer settings are so adjusted that at their lower end the desired voltage corresponding to the precipitation occurring in the time interval is supplied to the main program. When the computer control is in operating position, the relay mechanism automatically switches the mechanical wipers from one pot to the other at one second intervals so that the desired input rate curve is obtained. Although this is capable of reasonable accuracy, the limitations imposed in frequency response by the inertia of the relays and other moving parts must not be ignored. Another limitation, basic to the accuracy of the computer solution, is the number of step pots available on the device, because this limitation usually determines the time scaling of the problem.

## Interception

The expression for capacity interception rate is given by the equations:

$$i_{cc} = i e^{-P/S_I} \quad (4.1)$$

$$\text{with } i_{ca} = i \text{ for } i < i_{cc}$$

$$\text{and } i_{ca} = i_{cc} \text{ for } i > i_{cc} \quad (4.2)$$

The computer program for generating Equation 4.1, and the conditions defined by Equation 4.2, is represented by Figure 4.2.

In order to generate the function  $100e^{-P/S_I}$  the following procedure is adopted.

$$\begin{aligned} \text{Let } y &= 100e^{-P/S_I} \frac{dy}{dt} \\ &= -\left(\frac{100}{S_I}\right) (e^{-P/S_I}) \left(\frac{dP}{dt}\right) = -\left(\frac{i}{S_I}\right) y \quad (4.3) \end{aligned}$$

In other words  $y = 100e^{-P/S_I}$  will be the solution of the differential Equation 4.3. In Figure 4.2, the inputs A, B, and C into the multiplier 1 are:

$$\begin{aligned} A &= -i \\ B &= C = y \end{aligned}$$

so

$$AC = +iy/100$$

The input to amplifier 11,  $I_{11}$ , is given by:

$$I_{11} = +\frac{iy}{100} \frac{k}{S_I}$$

and

$$I_1 = +\frac{iy}{100} \frac{50k}{S_I} \quad (4.4)$$

$$\text{Thus, if } k = 2, I_1 = +\frac{iy}{S_I} = -\frac{dy}{dt}$$

The output of integrator 1, thus, will be:  $I_1 dt = -\int dy/dt dt = y$

The initial condition on integrator 1 can be set to represent the antecedent watershed conditions by adjusting the setting of potentiometer 17 (Figure 4.1). If there

has been no rain on the watershed for some days prior to the storm event, the watershed can be assumed to be dry. This means that the capacity interception rate can be assumed to commence from its maximum value and so the setting on Pot 17 will be 1.0. On the other hand, if there has been prior rain on the watershed, the interception capacity rate can be assumed to commence at a value below the maximum on the capacity rate curve. The setting on Pot 17 will therefore be less than one.

Because of the introduction of diode,  $D_1$ , in the feed back circuit of summing amplifier 15, its output,  $i_1 = i(1 - e^{-P/S})$  (Figure 4.1) will always be positive, which ensures the conditions required by Equation 4.12.

### Infiltration

The equations for infiltration capacity rate are given by:

$$f = f_c + (f_o - f_c) e^{-k_f/t} \quad \dots (4.5)$$

$$\begin{aligned} \text{with } f_a &= i_1 \text{ for } i_1 < f \\ \text{and } f_a &= f \text{ for } i_1 > f \quad \dots (4.6) \end{aligned}$$

Equation 4.5 along with the conditions defined by 4.6, are represented by Figure 4.3.

The output of amplifier 25 is  $f$ . Diode  $D_2$  provides for the boundary conditions given by Equation 4.6.

### Depression Storage

The equations for rate of inflow into depression storage are given by:

$$\sigma_c = i_2 e^{-(P_1 - F)/S_D} \quad \dots (4.7)$$

$$\begin{aligned} \text{with } \sigma_a &= i_2 \text{ when } \sigma_c > i_2 \\ \text{and } \sigma_a &= \sigma_c \text{ when } \sigma_c < i_2 \quad \dots (4.8) \end{aligned}$$

The computer program for these expressions is given by Figure 4.4. This circuit is similar to Figure 4.2, since Equations 4.7 and 4.1 are similar.

### Routing the Rainfall Excess

The expression that governs the routing of rainfall excess is given by:

$$p_e - Q = t_R \frac{dQ}{dt} \quad \dots (4.9)$$

or

$$\frac{dQ}{dt} = (p_e - Q)/t_R \quad \dots (4.10)$$

The analog circuit diagram for Equation 4.10 is shown by Figure 4.5.

### Time Scaling

The frequencies occurring in the problem solutions, the voltage levels present on the computer amplifiers, and the time required to obtain the solution of a problem, are all controlled by the proper choice of time and amplitude scale factors.

The mathematical equations involved in the present problem are exponential in nature and, therefore, do not pose any major difficulties associated with the frequency response type solutions. It would thus seem apparent that the time scaling of the problem will depend upon the nature of the input function.

The function input to the model is a step function of the precipitation, where each step represents the amount of rainfall occurring in that period of specified duration,  $\Delta t$ . The relay mechanism of the analog computer switches from one step to the other at an exact interval of one second. This means, that, if  $\Delta t$  is selected to be 10 minutes, then the time scale of the problem will be one second of computer time equalling 10 minutes of the real time. From the standpoint of computation accuracy, it is desirable that the value of  $\Delta t$  is as small as possible, and this increases the solution time on the computer. Riley, et al. (1967) used a value of  $\Delta t$  equal to five minutes in their studies on the modeling of Walnut Gulch watershed in Arizona where most of their storm durations are 60 minutes or less. The input device for the analog computer used in their study, like that of the study described by this report, has a maximum of 12 steps. This limitation suited the requirements on the Walnut Gulch watershed. However, the majority of the storms on the Waller Creek watershed (Austin, Texas) are of 360 minutes duration and some exceed this value. Further, the various statistical equations for the unit hydrograph characteristics of this watershed were developed for 30 minute durations (Espey, Jr., et al. 1965). Therefore, a value of  $\Delta t$  equal to 30 minutes is adopted as a convenient time scale for this study. This time scale permits the direct use of the rise time of Espey's unit hydrograph as the characteristic time ( $t_R$ ) in the routing of precipitation excess ( $p_e$ ) and also is adequate to model most of the storms of 360 minutes or less duration that occurred on the watershed with the number of steps available on the computer.



## Amplitude Scaling

The choice of a proper amplitude scale factor for a problem is as important as the choice of time scale. Amplitude scaling is done with the following considerations.

1. Voltage levels throughout the computer are to be maintained at an optimum value. The normal operating range of the computer is  $\pm 100$  volts. An attempt is, therefore, made to keep all peak voltages close to 100 volts, at the same time ensuring that very low maximum voltage levels are avoided.

2. The relation between the physical and the analog systems is preserved so that easy conversion of the voltages of the analog system into physical units is possible.

From a study of the precipitation data from the Waller Creek watershed, the maximum value of precipitation occurring in any 30 minute interval has been found to be 2.26 inches (occurred on May 16, 1965). In order to keep the peak voltage of the input close to 100 volts, a scale of 1 inch equal to 40 volts is selected, so that the maximum input voltage in any step of the input device will not exceed 90.4 volts. This amplitude scale is well suited to the problem as detailed on the next page.

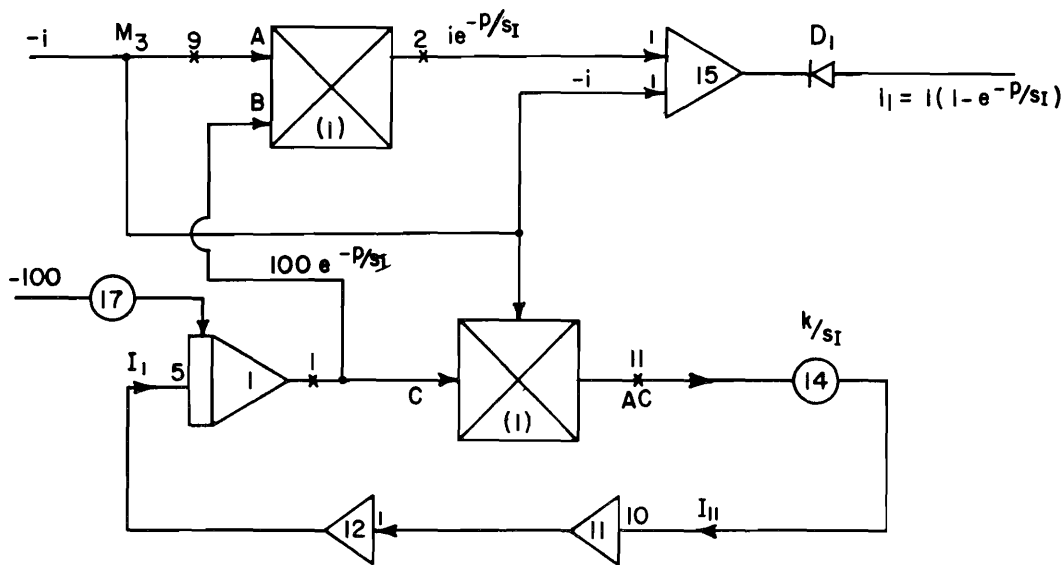


**Figure 4.2.** Analog circuit for generating the expression for interception rate.

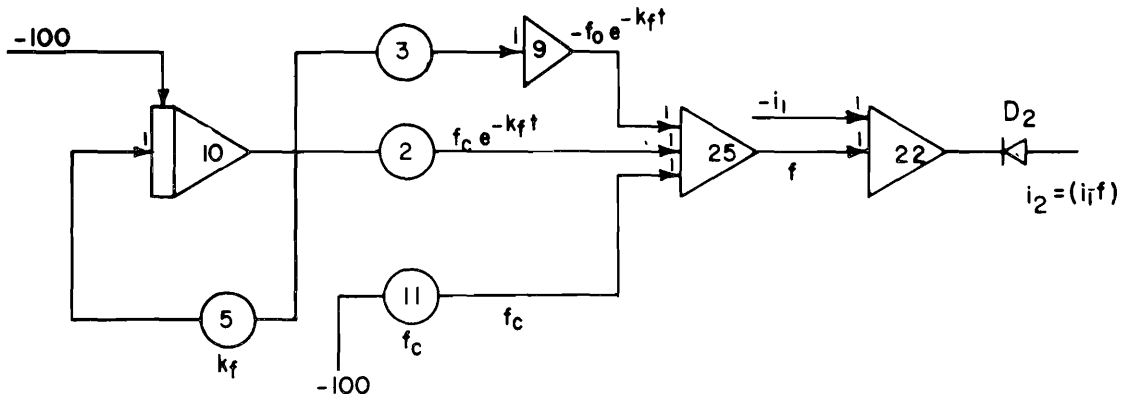


**Figure 4.3.** Analog circuit for generating the expression for infiltration rate.

## Interception

The physical units of interception storage are in inches. The amplitude scale is 1 inch equal to 40 volts. Computer value of precipitation in any time step  $C_i = 40i$ . Hence in Figure 4.2

$$A = -40i \text{ volts}$$

$$B = C = 100e^{-P/S_I}$$

$$I_{11} = \frac{+(40i)(100e^{-P/S_I})}{100} \times \frac{k}{40S_I}$$

$$I_1 = \frac{+(40i)(100e^{-P/S_I})}{100} \times \frac{k}{40S_I} \times 50$$

Since  $k = 2$

$$I_1 = \frac{(40i)(100e^{-P/S_I})}{(40S_I)}$$

Hence the scale for  $S_I$  is given by:

$$\frac{1}{20S_I} = \text{reading on Pot 14, } P_{14}$$

or

$$S_I = \frac{1}{20(P_{14})} \dots \dots \dots (4.11)$$

The maximum value of voltage on integrator 1 (Figure 4.1) will not exceed 100, since  $e^{-P/S_I}$  will always be less than or equal to one. Similarly, the maximum value of voltage on amplifier 15 (Figure 4.2) will not exceed 100 volts.

## Infiltration

The physical units of infiltration rates are in inches/hour. The corresponding computer units are volts/seconds. The physical values of  $f$  in the study do not exceed one inch per hour. This means that the value of the infiltration rate,  $f$ , on the computer will not exceed 20 volts per second.

## Depression storage

Since the circuit (Figure 4.4) for depression storage is almost the same as that for the interception, (Figure 4.2) the conversion factor for  $S_D$  in inches is given by:

$$S_D = \frac{1}{20 \times P_6} \dots \dots (4.12)$$

where

$P_6$  = reading of potentiometer 6 in Figure 4.3

## Routing of rainfall excess

The setting on Pot 7 (Figure 4.5) should be the converted value of the rise time of the unit hydrograph. For example, if rise time,  $t_R$ , of the unit hydrograph is 30 minutes, then the setting on Pot 7 is 30/30 or 1.0, and if it is 60 minutes, the corresponding setting is 30/60 or 0.5.

A possible source of overloading amplifier 18 (Figure 4.5) is when the precipitation excess is greater than 10 volts and when there is no runoff outflow. In such cases, the input of  $p_e$  to amplifier 18 may be wired with a gain of either 5 or 1. This gives outflow values of 5Q or Q respectively instead of 10Q. The output of amplifier 5, when input to an integrator, yields the total outflow for the storm.

## Outflow rate

The physical unit of outflow rate is cubic feet per second. The corresponding unit on the computer is volts per second of the computer time. The computer value of the output,  $Q_C$ , is converted to the physical units of outflow in the following manner:

Let  $Q_C$  be the output of amplifier 5 (Figure 4.5) and  $A$  be the area of the watershed in square miles.

Then the outflow rate,  $Q$ , in cfs is given by:

$$Q \text{ in cfs} = \frac{Q_C \times A \times 640 \times 43560}{10 \times 40 \times 30 \times 60 \times 12}$$

$$= 3.25 \times A \times Q_C \dots \dots \dots (4.13)$$

The areas of the 23rd and 38th Street watersheds are 4.0 and 2.26 square miles respectively. Substitution of these values in Equation 4.13 yields the following expressions for  $Q$  from 23rd and 38th Street watersheds.

$$Q \text{ for 38th Street in cfs} = 7.29 Q_C (4.14)$$

$$Q_T = \frac{Q_{TC} \times A \times 640}{10 \times 40 \times 12}$$

$$= .1333 \times A \times Q_{TC} \dots \dots (4.15)$$

### Total volume of outflow

The total volume of outflow,  $Q_{TQ}$ , is generally expressed as acre feet. The corresponding unit on the computer is volts. The computer value of the total volume of outflow,  $Q_{TC}$ , as indicated by the output of integrator 14 (Figure 4.5) is converted to the physical units in the following manner:

$$Q_T \text{ for 23rd Street in acre feet} = .533Q_{TC} \quad \dots \dots \dots (4.16)$$

$$Q_T \text{ for 38th Street in acre feet} \\ = .301Q_{TC}$$

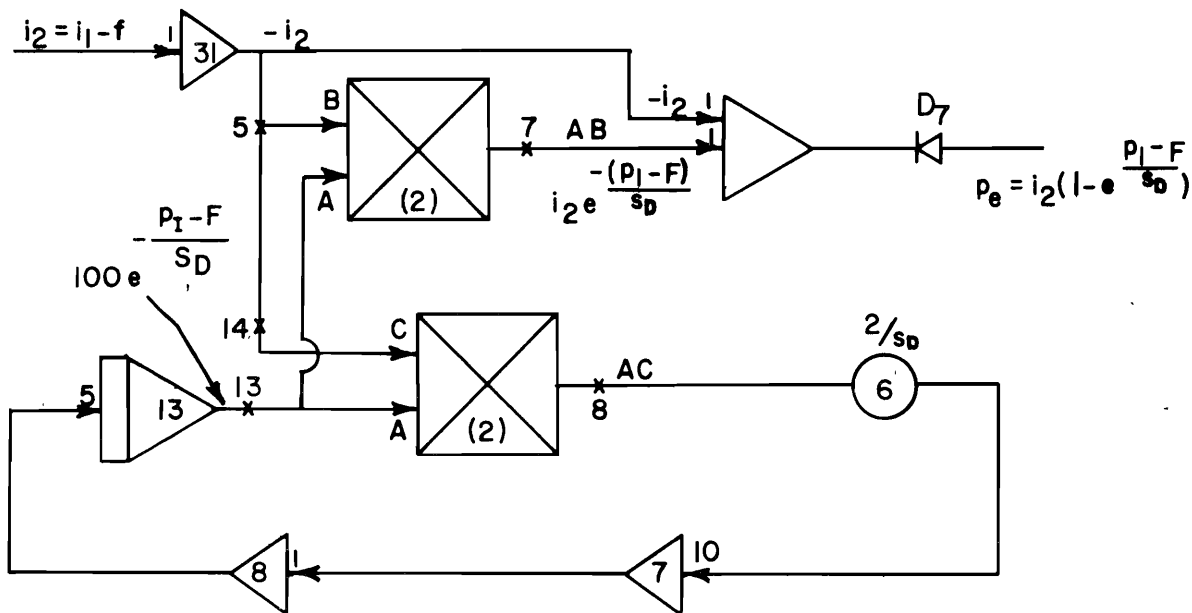


**Figure 4.4. Analog circuit for generating the expression for inflow rate in to depression storage.**

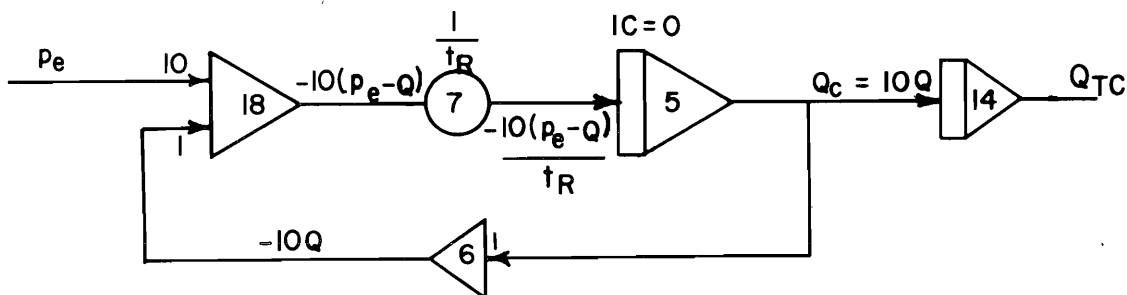


**Figure 4.5.** Analog circuit for obtaining the outflow hydrograph.

The scale factors for conversion of the physical variables to the computer variables and vice versa are summarized in Table 4.1.

Table 4.1. Scale factors relating the physical and computer variables.

Particulars	Pot or Amplifier in the Program (Figure 4.1)	Computer Values	Actual Values
Time scale		1 sec	30 min
Amplitude scale		40 volts	1 in
Interception Storage ( $S_I$ )	Pot 14	$P_{14}$	$\frac{1}{20 \times P_{14}}$ in
Infiltration $f_o$ Rates	Pot 3	$P_3$	$\frac{2P_3}{40}$ in/hr
$f_c$	Pot (2), Pot 11	$P_2$	$\frac{2P_2}{40}$ in/hr
$k_f$	Pot 4	$P_4$	$P_4$
Depression storage ( $S_D$ )	Pot 6	$P_6$	$\frac{1}{20 \times P_6}$ in
Rise time ( $t_R$ )	Pot 7	$P_7$	$\frac{30}{P_7}$ min
Outflow rate (Q) (23rd Street)	Amplifier 5	$Q_C$ volts/30 min	$Q_C \times 12.9$ cfs
(38th Street)	Amplifier 5	$Q_C$ volts/30 min	$Q_C \times 7.29$ cfs
Outflow total ( $Q_T$ ) (23rd Street)	Amplifier 14	$Q_{TC}$ volts	$Q_{TC} \times .533$ ac-ft
(38th Street)	Amplifier 14	$Q_{TC}$ volts	$Q_{TC} \times .301$ ac-ft



## CHAPTER V MODEL VERIFICATION

In applying the mathematical model of a rural watershed to a given urban watershed, consider the concept of a rural watershed which is equivalent to the given rainfall hydrograph. This imaginary watershed, termed "equivalent rural watershed," is assumed to possess certain geometric and physical characteristics. These characteristics depend upon the urban parameters which vary from year to year in any urban watershed. The object of the model verification study is to define these characteristics from year to year by simulating several runoff events with the mathematical model on the analog computer, and thus to develop acceptable relations between the urban parameters and the watershed characteristics.

### Geometric Characteristics of the Watershed

The geometric characteristics of the equivalent rural watershed may be represented by its area,  $A_{ER}$ , maximum length of travel,  $L_{ER}$ , and mean slope,  $S_{ER}$ . These can be determined from the assumption that the unit hydrograph characteristics of both the urban and its equivalent rural watershed are identical. Equations 2.4 and 2.7 are derived from this assumption. These expressions include parameters such as rise time,  $t_R$ , maximum length of travel,  $L$ , and mean slope of the watershed,  $S$ , for the given urban watersheds. Using the appropriate values of percentage impervious cover,  $C_f$ , and the mean characteristic impervious length,  $L_m$ , (Table 3.4) and Equations 2.4 and 2.7, a digital computer program (Appendix B) was developed to obtain the characteristics of the unit hydrographs, length, area, and the slope of the equivalent rural watershed at various stages of urban development.

The area of the equivalent rural watershed,  $A_{ER}$ , is determined by equating the expression for  $Q_0$ ,  $W_{50}$ ,  $W_{75}$ , and  $T_B$  (Table 2.1) of the rural watershed unit hydrograph with those of the unit graph for the urban watershed. The four values of  $A_{ER}$  thus obtained are averaged. The mean area of the equivalent rural watershed did not differ from the area of the given urban watershed. The major changes of geometry, resulting from the transformation to the equivalent rural watershed, are in the maximum length of travel and the mean slope of the watershed.

The geometric characteristics  $L_{ER}$  and  $S_{ER}$  are functions of the degree of urbanization on the watershed. Relationships developed between these variables are shown by Figures 5.1 and 5.2. These figures indicate the following effects of urban trends on the geometric and the unit hydrograph characteristics of the watershed.

1. The maximum length of travel,  $L_{ER}$  is shortened by more than 60 percent in the equivalent rural watershed.
2. The slope of the equivalent rural watershed,  $S_{ER}$  is steepened.
3. The rise time,  $t_{RU}$ , is shortened, while the peak discharge rate,  $q_p$ , is increased by nearly 27 percent.

The output of the computer program (Appendix B) further indicated that the widths of the unit hydrograph (at the base, at 50 percent peak, and at 75 percent peak) are reduced with increase in urbanization.

The observations of the preceding paragraphs are significant in explaining the hydrologic behavior of an urban watershed (such as increase in peak rate and volume of outflow, and reduction in the values of rise time) in terms of changes in the geometric characteristics of the equivalent rural watershed. For instance, urban growth increases the value of  $C_f$ , which in turn reduces the average infiltration rate on the equivalent rural watershed. Geometrically, the equivalent rural watershed becomes shorter and steeper with increasing urbanization on a given watershed (Appendix B). The velocity and the volume of flow on the equivalent rural watershed is increased due to the reduction in both infiltration rate and length of travel and the increase in the mean slope of the watershed. These reasons logically explain why urban development on any watershed produces higher peak rates and volumes of outflow, and lower rise time and other time parameters. Figures 5.1 and 5.2 also indicate that the percentage impervious cover parameters,  $C_f$ , influences the values of the characteristics  $t_R$ ,  $q_p$ ,  $L_{ER}$ , and  $S_{ER}$  throughout the entire range of  $C_f$  considered in the study. On the other hand, when an approximate limiting value of the characteristic impervious length factor,  $L_f$ , is reached, the slopes of the curves plotted as functions of this parameter increase sharply. At this point,  $L_f$ , ceases to appreciably influence the plots and further variation of the dependent functions is produced by the percentage impervious cover parameter,  $C_f$ .

### Physical Characteristics of the Watershed

The physical characteristics or watershed coefficients of the equivalent rural watershed depend upon the urban parameters of the prototype which vary from year to year. These coefficients are represented by interception storage capacity  $S_t$ , the maximum infiltration capacity rate,  $f_o$ , the minimum infiltration capacity rates,  $f_c$ , and the exponential decay factor,  $k_f$ , in Horton's infiltration

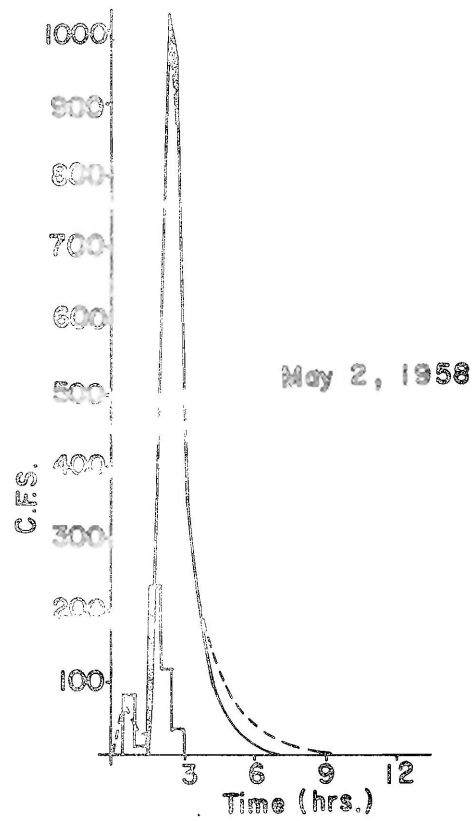
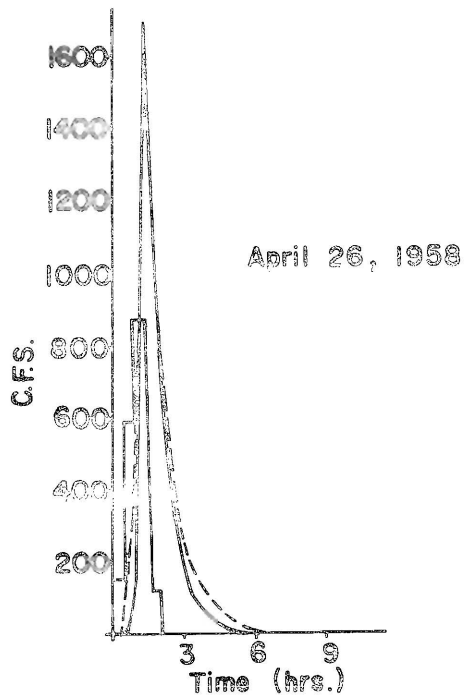
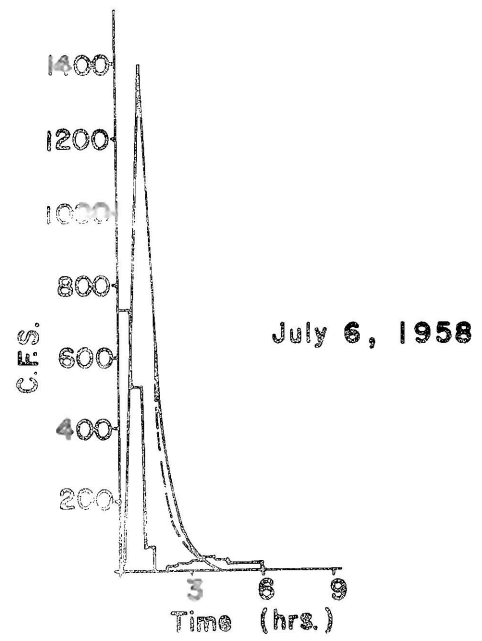
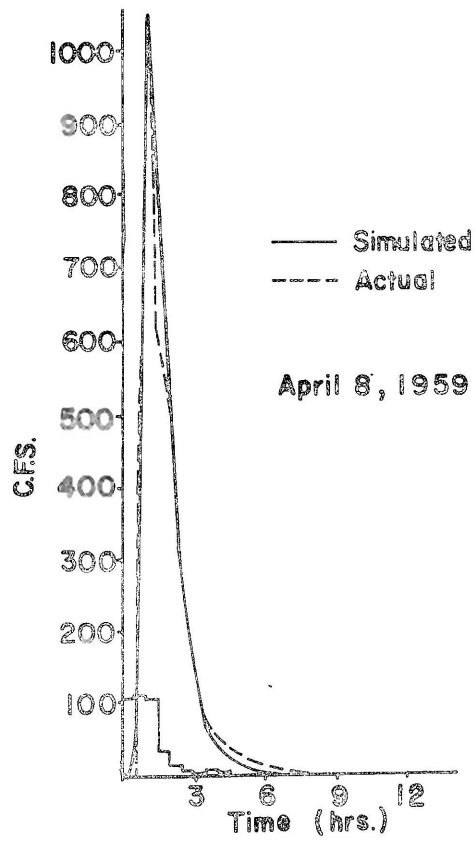


Figure 5.3. Comparison between the simulated and actual hydrographs.

**Table 5.1. Characteristics of simulated and actual outflow hydrograph for the Waller Creek watershed.**

Date <sup>4</sup>	Peak rate of outflow		Rise time for the peak		Total values of outflow		Total duration of outflow		Timelag	
	$Q_p$		$T_R$		$Q_T$		$T_D$		$T_L^3$	
	cfs		min.		acre feet		min.		min.	
	sim. <sup>1</sup>	obs. <sup>2</sup>	sim.	obs.	sim.	obs.	sim.	obs.	sim.	obs.
23rd Street										
010556	640	620	84	72	128	121	480	480	72	126
010556	340	385								
200357	1100	1200	32	33	97	96	720	735	0	0
260557	1080	1090	90	90	134	97	396	432	63	72
120657	1980	2050	75	72	320	298	432	460	18	15
120657	1012	1080	162	165						
220957	310	340	30	25	32	25	324	324	22	45
260458	1680	1700	69	62	189	198	342	414	40	45
020558	1006	1010	40	32	174	207	324	324	54	48
020558	452	410	63	60			302	228	18	20
060758	1360	1330	54	60	107	120	288	306	9	9
080459	1100	1080	72	72	122	125	342	360	22	28
110459	190	191								
240659	152	153	36	30	44	69	324	360	15	18
240659	219	222								
230959	1920	1915	45	45	171	143	288	360	36	28
031059	348	390	33	30	344	323	288	288	10	15
240660	192	192	30	80	108	76	396	396	84	90
240660	155	152								
240660	90	84								
240660	374	360								
161060	1020	1020	81	82	105	91	450	504	68	60
281060	1685	1600	52	45	175	206	270	270	234	234
281060	3819	3825	114	90	554	575	432	432		
160261	870	870	45	45	171	207	540	630	18	20
090761	2275	2163	148	135	299	299	360	396	270	240
090761	697	693								
010662	271	200	22	38	22	30	22	38	260	360
020662	258	252	40	38	28	28	300	324	0	0
030662	2580	2270	72	72	247	213	713	720	54	45
100662	1858	1700	68	68	192	214	342	360	90	95
250862	1910	1980	54	45	277	236	432	500	10	12
060962	468	470	32	36	28	34	225	260	12	15
070962	813	800	68	60	98	109	486	486	18	15
011062	916	930	36	30	60	65	756	756	15	8
081062	595	590	72	75	70	90	378	360	36	30

<sup>1</sup>sim. denotes simulated.

<sup>2</sup>obs. denotes observed.

<sup>3</sup> $T_L$  denotes time lag which is defined in this analysis as the difference in time between the commencement of the storm precip and the storm outflow.

<sup>4</sup>The order of the date, month, and year. Eg: 010556 means 1st May, 1956.



Table 5.1. Continued.

Date	$Q_p$ cfs		$T_R$ min.		$Q_T$ acre feet		$T_D$ min.		$T_L$ min.	
	sim.	obs.	sim.	obs.	sim.	obs.	sim.	obs.	sim.	obs.
23rd Street										
180364	740	839	45	45	89	79	360	396	27	22
160964	160	140	27	30	10	16	216	195	180	190
270964	2320	2280	108	105	328	355	414	496	108	105
210165	516	545	180	180	68	69	486	486		
160265	606	600	184	195	116	171	641	630		
160565	2280	2320	26	30	247	248	306	324	0	15
180565	1980	2000	57	75	222	240	288	324	90	72
38th Street										
010556	108	108	120	45	17	37	630	630		
120657	520	500	45	45	111	115	645	660		
220957	160	156	30	38	20	30	525	525		
131057	370	370	285	270	72	104	765	757		
260458	460	465	75	75	52	69	517	520		
020558	252	276	45	60	33	53	520	525		
060758	474	500	45	30	54	45	540	580		
080459	240	230	67	70	36	42	540	540		
230959	485	470	54	60	60	58	495	540		
161060	240	230	72	60	30	38	520	540		
160261	395	355	45	60	87	93	765	765		
030662	760	805	65	62	93	94	710	725		
100662	1440	1420	150	152	180	147	520	520		
240862	620	620	105	105	111	99	520	520		
070962	460	430	63	75	54	63	585	600		
081062	255	215	60	75	36	34	625	630		
160664	610	580	75	90	121	157	750	740		
270964	1320	1320	115	120	180	175	460	480		
160565	820	805	28	28	62	97	365	365		
180565	790	790	70	105	80	99	435	495		

**Table 5.2. Regression between actual and simulated hydrograph characteristics.**

No.	Parameter	Number of observations	Regression Equation <sup>3</sup>	R	R <sup>2</sup>	
1.	a <sup>1</sup>	Q <sub>p</sub>	63	Q <sub>p</sub> <sup>1</sup> = 1.981 + 1.015Q <sub>p</sub>	.995	.991
	b <sup>2</sup>	Q <sub>p</sub>	63	Q <sub>p</sub> <sup>1</sup> = 8.570 + 1.007Q <sub>p</sub>	.992	.983
2.	a	T <sub>R</sub>	56	T <sub>R</sub> <sup>1</sup> = -2.561 + 1.032T <sub>R</sub>	.973	.947
	b	T <sub>R</sub>	56	T <sub>R</sub> <sup>1</sup> = -1.393 + .978T <sub>R</sub>	.947	.897
3.	a	Q <sub>T</sub>	54	Q <sub>T</sub> <sup>1</sup> = +3.750 + 0.971Q <sub>T</sub>	.984	.968
	b	Q <sub>T</sub>	54	Q <sub>T</sub> <sup>1</sup> = +9.349 + .940Q <sub>T</sub>	.967	.938
4.	a	T <sub>D</sub>	55	T <sub>D</sub> <sup>1</sup> = -21.546 + 1.010T <sub>D</sub>	.992	.984
	b	T <sub>D</sub>	55	T <sub>D</sub> <sup>1</sup> = -14.128 + .995T <sub>D</sub>	.984	.969
5.	a	T <sub>L</sub>	32	T <sub>L</sub> <sup>1</sup> = 1.568 + .908T <sub>L</sub>	.985	.971
	b	T <sub>L</sub>	32	T <sub>L</sub> <sup>1</sup> = 3.306 + .881T <sub>L</sub>	.971	.943

<sup>1</sup> a - By the procedure of minimizing the square of normal deviations.

<sup>2</sup> b - By the ordinary least square procedure.

<sup>3</sup> The superscript on the left hand term denotes a simulated value of the parameter.

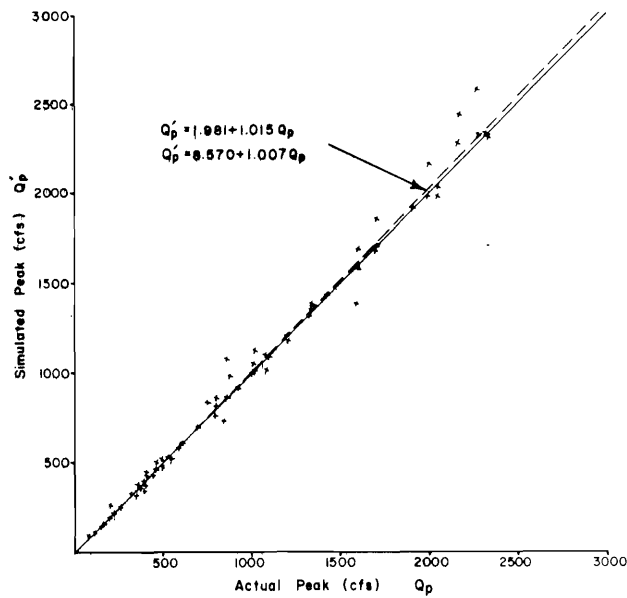


Figure 5.4. Comparison of the simulated and actual values of peak rate of outflow.

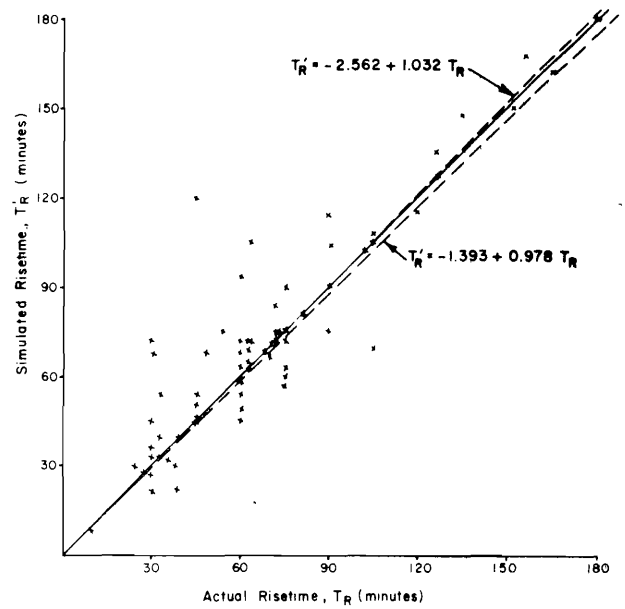


Figure 5.6. Comparison of the simulated and actual values of the total volume of outflow.

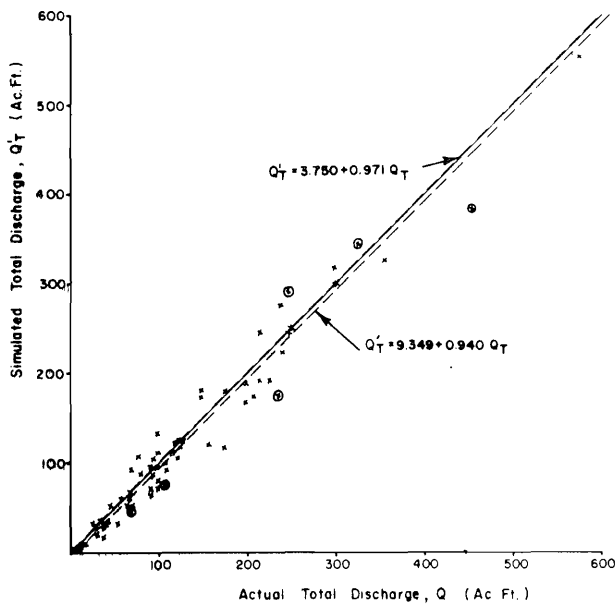


Figure 5.5. Comparison of the simulated and actual values of the rise time of the hydrograph.

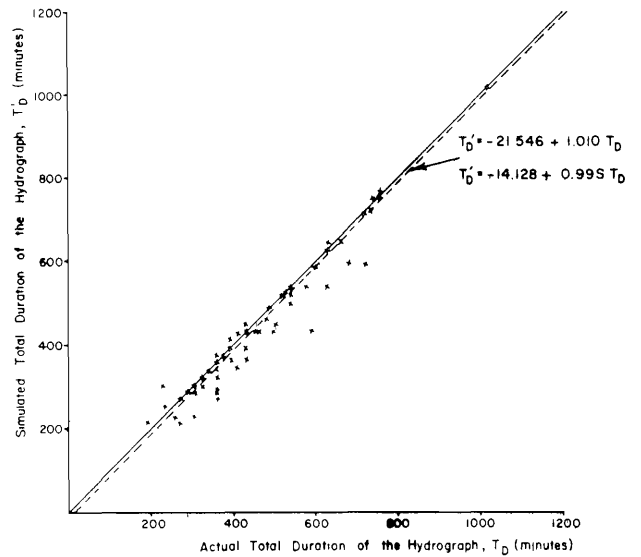


Figure 5.7. Comparison of the simulated and actual values of total duration of the hydrograph.



## CHAPTER VI MODELING RESULTS

Simulation models of the hydrologic processes occurring within an urbanized area have a wide variety of useful applications. In this chapter, the hydrologic model of the Waller Creek watershed is used to establish relationships between watershed coefficients, such as interception storage capacity and maximum infiltration capacity rate, and the urban parameters applied in the model. In addition, sensitivity studies are discussed whereby the model is used to demonstrate the relative influences of various parameter and processes upon the operation of the hydrologic system as a whole.

### Relation Between Watershed Coefficients and Urban Parameters

Data reported in Table 6.1 have been statistically analyzed to relate each of the individual watershed coefficients with the urban parameters  $C_f$  and  $L_f$ . The interpretation of the results of statistical analysis is discussed in the following paragraphs.

#### Interception storage capacity

Attempts to relate by multiple regression the interception storage capacity,  $S_i$ , with percentage impervious cover,  $C_f$ , and characteristic impervious length factor,  $L_f$ , yielded promising results. The following models were tested.

- 1)  $S_i = b_0 + b_1 C_f + b_2 L_f$
- 2)  $S_i = b_0 + b_1 \log C_f + b_2 \log L_f$

The coefficients of regression for various models relating  $S_i$  with  $C_f$  and  $L_f$  are presented in Table 6.3. An analysis of variance for each of the models is presented in Tables 6.4 and 6.5. The low value of the mean squares due to residuals in the tables indicates that interaction between the independent variables is relatively small. The F-test (Table 6.4) and the values of  $R$  and  $R^2$  for both models (Table 6.3) indicate that model 1 provides a better correlation between the variables than model 2.

A comparison of the values of the interception storage capacity,  $S_i$ , derived from the analog computer simulation study (Table 6.1) and those computed from the regression equation of model 1 (Table 6.3) is presented in Table 6.6. The relationship between the actual (simulated) and statistically estimated values of  $S_i$  is shown by Figure 6.1.

#### Maximum and minimum capacity rates

Maximum,  $f_o$ , and minimum,  $f_c$ , infiltration capacity rates in Horton's infiltration equation are found to be highly correlated by a linear model of the form  $f_o = b_0 + b_1 C_f + b_2 L_f$ . The results of the statistical analysis are presented in Tables 6.7, 6.8, and 6.9. The analysis of variance (Tables 6.8 and 6.9) indicates that the linear models adopted (Table 6.7) are adequate for statistically relating the capacity rates of infiltration with the two urban parameters. Further, the T-tests in the analysis points out that both  $C_f$  and  $L_f$  equally affect the infiltration rates. As in the analysis for  $S_i$ , the values of the mean squares for the residuals are relatively low. This confirms the relative independence of  $C_f$  and  $L_f$ . The regression equation also indicates that urban growth as characterized by increases in the values of both  $C_f$  and  $L_f$  reduces infiltration rates. This is one of the reasons why urban development produces increased flood peaks and volumes.

Comparison of the estimated (using statistical models in Table 6.7) and actual (simulated) values of  $f_o$  and  $f_c$  are reported in Tables 6.10 and 6.11 respectively.

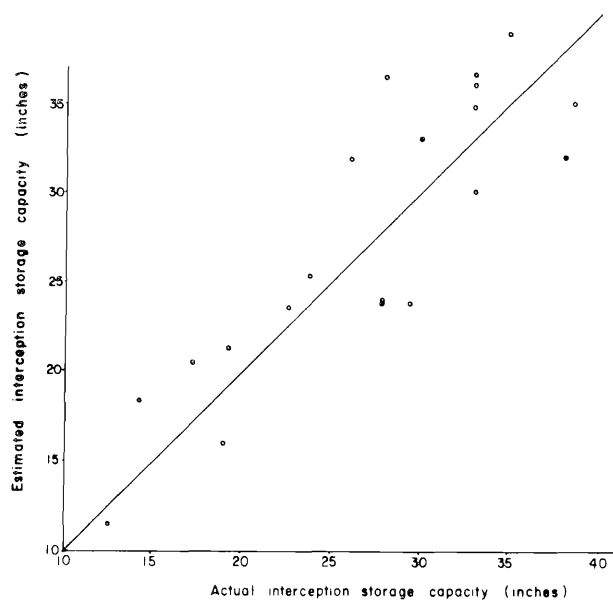


Figure 6.1. The relationship between the actual and the estimated interception storage capacity.

**Table 6.7. Linear correlation of maximum and minimum infiltration capacities with the urban parameters.**

Parameter	No. of Observations	Regression Equation	R	R <sup>2</sup>
$f_o$	40	$f_o = 2.029 - 2.986C_f - 1.141L_f$	.891	.794
$f_c$	40	$f_c = 1.066 - 1.222C_f - 0.973L_f$	.747	.558

**Table 6.8. Analysis of variance for relating maximum infiltration capacity rate with the urban parameters.**

Source	Degrees of Freedom	Sum of Squares	Mean Squares	Standard Error	Tests
Due to regression	2	.317	.159		F-71.41
Due to $C_f$	1		.197	.317	T- 9.41
Due to $L_f$	1		.063	.264	T- 5.31
Due to residuals	37	.082	.022		
Total	39	.399			

**Table 6.9. Analysis of variance for relating minimum infiltration capacity rate with the urban parameters.**

Source	Degrees of Freedom	Sum of Squares	Mean Squares	Standard Error	Tests
Due to regression	2	.079	.039		F-23.32
Due to $C_f$	1		.033	.277	T- 4.41
Due to $L_f$	1		.030	.231	T- 4.20
Due to residual	37	.063	.002		
Total	39	.141			

Table 6.10. Comparison of the actual and estimated maximum infiltration capacity rates.

No.	Actual $f_o$ in/hr.	Estimated $f_o$ in/hr.	Difference in/hr.
1	.1800	.2602	-.0802
2	.2000	.2602	-.0602
3	.2000	.2602	-.0602
4	.2000	.2602	-.0602
5	.3000	.3190	-.0190
6	.3000	.3197	-.0197
7	.4000	.3459	.0541
8	.4000	.3459	.0541
9	.4000	.3723	.0276
10	.4400	.3197	.1202
11	.4500	.4111	.0389
12	.4500	.4111	.0389
13	.4500	.4111	.0389
14	.4800	.4415	.0385
15	.4800	.44156	.0385
16	.4600	.4724	-.0124
17	.4600	.4724	-.0124
18	.4500	.4724	-.0224
19	.4500	.5047	-.0547
20	.4500	.5047	-.0547
21	.4950	.5151	-.0201
22	.4500	.4343	.0157
23	.4500	.4015	.0485
24	.5000	.4015	.0985
25	.3750	.4015	-.0265
26	.3250	.3671	-.0421
27	.3250	.3671	-.0421
28	.3250	.3671	-.0421
29	.2750	.2997	-.0247
30	.2750	.2997	-.0247
31	.2750	.2997	-.0247
32	.2750	.2997	-.0247
33	.2750	.2997	-.0247
34	.2500	.2512	-.0012
35	.2500	.2512	-.0012
36	.2500	.2512	-.0012
37	.2500	.2512	-.0012
38	.2500	.2020	.0480
39	.2500	.2020	.0480
40	.2500	.2020	.0480

Table 6.11. Comparison of the actual and the estimated minimum infiltration capacity rates.

No.	Actual $f_c$ in/hr.	Estimated $f_c$ in/hr.	Difference in/hr.
1	.1300	.1643	-.0343
2	.1500	.1643	-.0143
3	.1500	.1643	-.0143
4	.1500	.1643	-.0143
5	.2400	.1910	.0490
6	.2400	.1915	.0490
7	.2000	.2026	-.0026
8	.2000	.2026	-.0026
9	.2000	.2140	-.0140
10	.3200	.1915	.1284
11	.2400	.2338	.0062
12	.2400	.2338	.0062
13	.2400	.2338	.0062
14	.3000	.2479	.0521
15	.3000	.2479	.0521
16	.2600	.2623	-.0023
17	.2600	.2623	-.0023
18	.2000	.2623	-.0623
19	.2000	.2777	-.0777
20	.2000	.2777	-.0777
21	.2800	.2613	.0187
22	.2600	.2227	.0373
23	.2500	.2086	.0414
24	.2900	.2086	.0814
25	.1800	.2086	-.0286
26	.2000	.1935	.0065
27	.2000	.1935	.0065
28	.2000	.1935	.0065
29	.1300	.1642	-.0342
30	.1300	.1642	-.0342
31	.1300	.1642	-.0342
32	.1300	.1642	-.0342
33	.1300	.1642	-.0342
34	.1300	.1429	-.0129
35	.1300	.1429	-.0129
36	.1300	.1429	-.0129
37	.1300	.1429	-.0129
38	.1300	.1225	.0075
39	.1300	.1225	.0075
40	.1300	.1225	.0075



Table 6.12. Coefficients of regression for various models relating depression storage capacity with the urban parameters.

Model	R	R <sup>2</sup>	Regression Equation
1	.772	.597	$S_D = -1.069 + 0.580C_f + 2.679L_f$
2	.631	.398	$S_D = 1.456 + 0.188 \log C_f + 2.911 \log L_f$

Table 6.13. Analysis of variance for depression storage capacity related to the urban parameters by the model 1.

Source	Degrees of Freedom	Sum of Squares	Mean Squares	Standard Error	Tests
Due to regression	2	.261	.131		F-27.36
Due to $C_f$	1		.007	.466	T- 1.25
Due to $L_f$	1		.227	.389	T- 6.89
Due to residuals	37	.177	.005		
Total	39	.438			

Table 6.14. Analysis of variance for depression storage capacity related to the urban parameters by the model 2.

Source	Degrees of Freedom	Sum of Squares	Mean Squares	Standard Error	Tests
Due to regression	2	.280	.140		F-14.87
Due to $C_f$	1		.002	.407	T- .46
Due to $L_f$	1		.272	.542	T- 5.38
Due to residuals	45	.424	.004	.009	
Total	47	.704			

Table 6.15. Comparison of the actual and the estimated depression storage capacity.

No.	Actual $S_D$ inches	Estimated $S_D$ inches	Difference inches
1	.4550	.3564	.0986
2	.4550	.3564	.0986
3	.4170	.3564	.0606
4	.3130	.3564	-.0434
5	.3570	.3286	.0284
6	.3570	.3273	.0297
7	.3570	.3198	.0372
8	.4170	.3198	.0972
9	.2770	.3113	-.0343
10	.3570	.3273	.0297
11	.2780	.2799	-.0019
12	.2780	.2799	-.0019
13	.2780	.2799	-.0019
14	.2500	.2639	-.0139
15	.2500	.2639	-.0139
16	.2000	.2473	-.0473
17	.2000	.2473	-.0473
18	.1390	.2473	-.1083
19	.2000	.2279	-.0278
20	.2000	.2279	-.0078
21	.2730	.3509	-.0779
22	.3800	.4000	-.0200
23	.6000	.4105	.1895
24	.6250	.4105	.2145
25	.4170	.4105	.0065
26	.4380	.4234	.0146
27	.4280	.4234	.0146
28	.4380	.4234	.0146
29	.4170	.4471	-.0301
30	.4170	.4471	-.0301
31	.4170	.4471	-.0301
32	.4170	.4471	-.0301
33	.4170	.4471	-.0301
34	.4550	.4654	-.0104
35	.4550	.4654	-.0104
36	.4550	.4654	-.0104
37	.4550	.4654	-.0104
38	.3850	.4764	-.0914
39	.3850	.4764	-.0914
40	.3850	.4764	-.0914

The coefficient of regression,  $R$ , is equal to .987, and  $R^2$  is equal to .973. The analysis of variance for relating  $t_R$  with  $C_f$  and  $L_f$  by Equation 6.1 is presented in Table 6.16.

The analysis presented by Table 6.16 indicates that  $L_f$  has relatively more effect on  $t_R$  than  $C_f$ . Using the regression Equation 6.1, it can be shown that (a) for a constant value of  $L_f$ , the value of  $t_R$  reduces with increase in  $C_f$ , and (b) for a constant value of  $C_f$ ,  $t_R$  increases directly with  $L_f$ . This result confirms the fact that urban

growth, as indicated by increases in  $C_f$ , reduces the value of  $t_R$ . For a particular level of urban development as indicated by a given value of  $C_f$  the rise time,  $t_r$ , is directly proportional to  $L_f$ .

Values for the rise time of the unit hydrograph derived from analog computer model verification studies are compared in Table 6.17 with those computed by Equation 6.1. The values of  $t_R$  adopted in the computer verification are the same as those computed from Espey's equations. The relationship between the actual values of

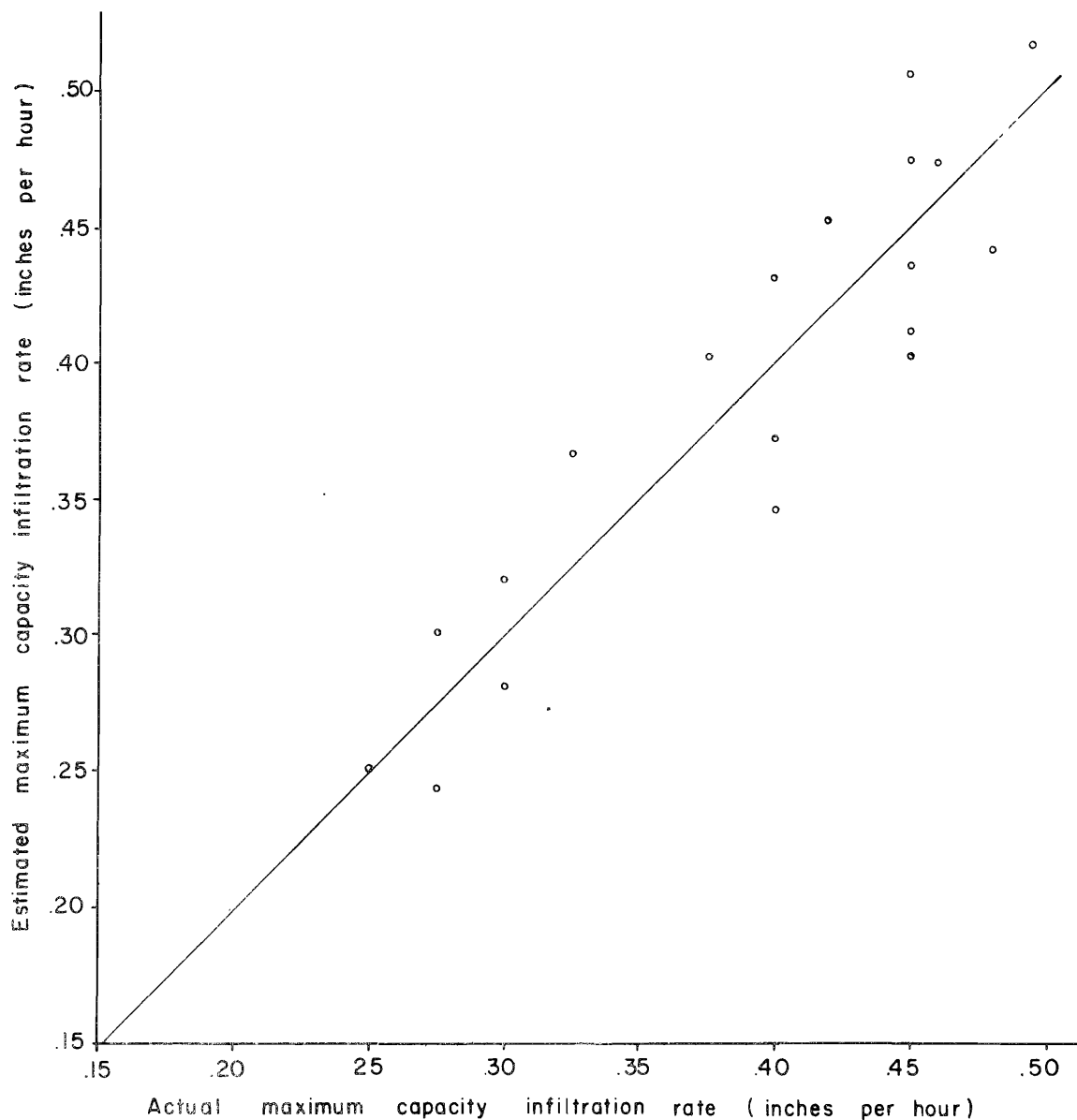
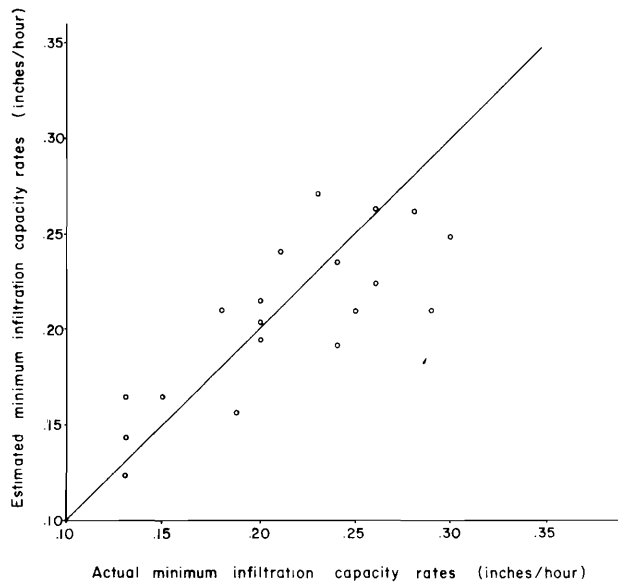


Figure 6.2. The relationship between the actual and the estimated maximum infiltration capacity rates.



**Figure 6.3. The relationship between the actual and estimated minimum infiltration capacity rates.**

$t_R$  (derived from analog computer model) and those estimated by Equation 6.1 are shown by Figure 6.5 along with the scatter from the equal-value line.

A word of caution is essential at this point, with regard to the general application of Equation 6.1 to other watersheds. The independent parameters,  $C_f$  and  $L_f$ , considered in the equation are non-dimensional, while the

dependent variable,  $t_R$ , has the dimension of minutes. This rules out, therefore, the general application of Equation 6.1 to watersheds of any size.

#### Adequacy of the regression equations

The regression equations for the watershed coefficients, derived in the previous sections as function of percentage impervious cover,  $C_f$ , and the characteristic impervious length factor,  $L_f$ , are summarized as follows:

$$S_I = -0.780 - 0.214C_f + 2.476L_f \quad (6.2)$$

$$f_O = 2.029 - 2.986C_f - 1.141L_f \quad (6.3)$$

$$f_C = 1.066 - 1.222C_f - 0.973L_f \quad (6.4)$$

$$S_D = -1.069 + 0.580C_f + 2.679L_f \quad (6.5)$$

$$t_R = 52.26 - 83.70C_f + 75.69L_f \quad (6.6)$$

The results presented thus far indicate that the above equations are adequate statistically in relating the watershed coefficients with the urban parameters.

The validity of the above expressions for predicting watershed coefficients, for various stages of urban development, is tested by applying the equations to both completely rural and urbanized watersheds. The assumed values of the parameters  $C_f$  and  $L_f$ , under these watershed conditions, are reported in Table 6.18. In the following

**Table 6.16. Analysis of variance for relating the rise time of the unit hydrograph with the urban parameters.**

Source	Degrees of Freedom	Sum of Squares	Mean Squares	Standard Error	Tests
Due to regression	2	279.35	139.68		F-672.39
Due to $C_f$	1		154.42	3.06	T-272.64
Due to $L_f$	1		181.18	2.56	T-295.33
Due to residuals	37	7.69	.207		
Total	39	287.04			

Table 6.17. Comparison between the actual and the estimated values of rise time of the unit hydrograph.

No.	Actual $t_R$ minutes	Estimated $t_R$ minutes	Difference minutes
1	54.93	54.45	.4809
2	54.93	54.45	.4809
3	54.93	54.45	.4809
4	54.93	54.45	.4809
5	55.57	55.32	.2546
6	55.57	55.28	.2924
7	55.80	55.90	-.0965
8	55.80	55.90	-.0965
9	56.02	56.48	-.4568
10	55.57	55.28	.2924
11	56.35	56.42	-.0721
12	56.35	56.42	-.0721
13	56.35	56.42	-.0721
14	56.71	56.79	-.0856
15	56.71	56.79	-.0856
16	56.91	57.15	-.2422
17	56.91	57.15	-.2422
18	56.91	57.15	-.2422
19	57.07	57.42	-.3522
20	57.07	57.42	-.3522
21	64.53	63.70	.8284
22	63.70	63.04	.6621
23	62.66	62.31	.3471
24	62.66	62.31	.3471
25	62.66	62.31	.3471
26	61.79	61.65	.1423
27	61.79	61.65	.1423
28	61.79	61.65	.1423
29	60.00	60.27	-.2650
30	60.00	60.27	-.2650
31	60.00	60.27	-.2650
32	60.00	60.27	-.2650
33	60.00	60.27	-.2650
34	58.45	59.33	-.8814
35	58.45	59.33	-.8814
36	58.45	59.33	-.8814
37	58.45	59.33	-.8814
38	58.55	58.02	.5290
39	58.55	58.02	.5290
40	58.55	58.02	.5290

Table 6.20. Actual values of the watershed coefficients.

Date	Watershed Coefficients				
	$S_I$ inches	$f_o$ inches/hour	$f_c$ inches/hour	$S_D$ inches	$t_R$ minutes
May 1, 1956	.143	.450	.200	.200	57.07
May 26, 1957	.125	.450	.200	.139	56.91

actually recorded. Sensitivity studies of the effects of each of the watershed coefficients on the outflow hydrograph are discussed in the following paragraphs.

#### Maximum capacity infiltration rate

The values of  $f_o^1/f_o$  and the corresponding  $Q_p^1/Q_p$  and  $Q_T^2/Q_T$  are presented in Table 6.21. The outflow hydrographs resulting from the various values of  $f_{or}$  are shown by Figures 6.6 and 6.7. Figure 6.8 represents the variation of the peak rate and total volume of outflow corresponding to variations in the maximum infiltration capacity.

The data reported in Table 6.21 and Figure 6.8 indicate that for the storm of May 1, 1956 when  $f_{or}$  is 15,  $Q_{pr}$  is equal to 0.3. For the second storm investigated (May 26, 1957) the corresponding  $Q_{pr}$  is 0.56. The corresponding values of  $Q_{Tr}$  for the two storms are 0.38 and 0.52 respectively. For values of  $f_{or}$  close to 1.0 (15 percent), the model is particularly insensitive to changes in this parameter.

In addition, variations in the maximum infiltration capacity rate produce relatively small changes in the values of both peak outflow rate and the total volume. This relative insensitivity of the model to the variations in  $f_o$  is due to (a) rapid transition from the maximum to the minimum infiltration capacity rate as indicated by the value of the decay constant,  $K_f(0.5)$  and (b) the small difference between the maximum and minimum infiltration capacity rates.

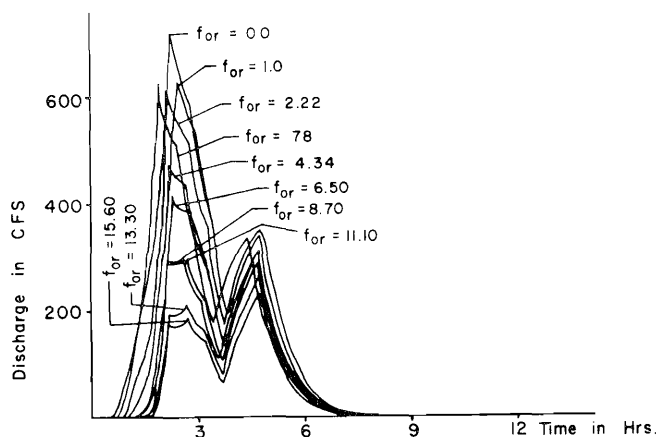


Figure 6.6. Outflow hydrographs resulting from the variation of  $f_o$  for the storm on 1 May 1956.

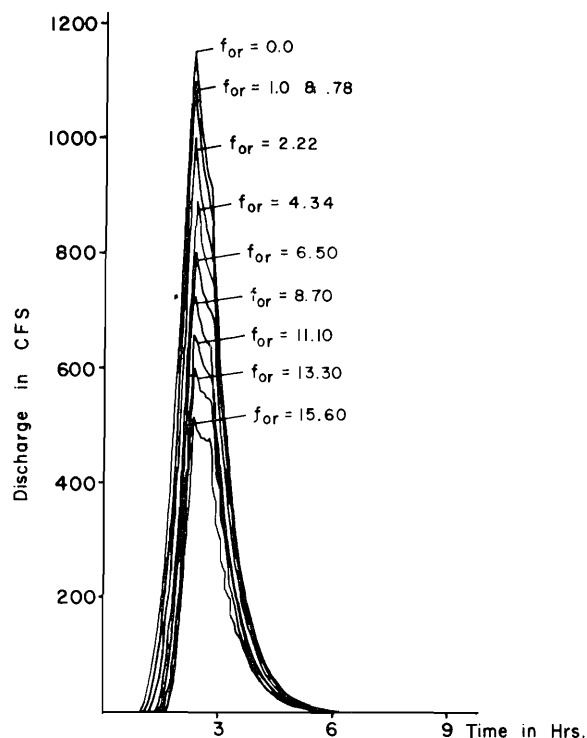


Figure 6.7. Outflow hydrographs resulting from the variation of  $f_o$  for the storm on 26 May 1957.

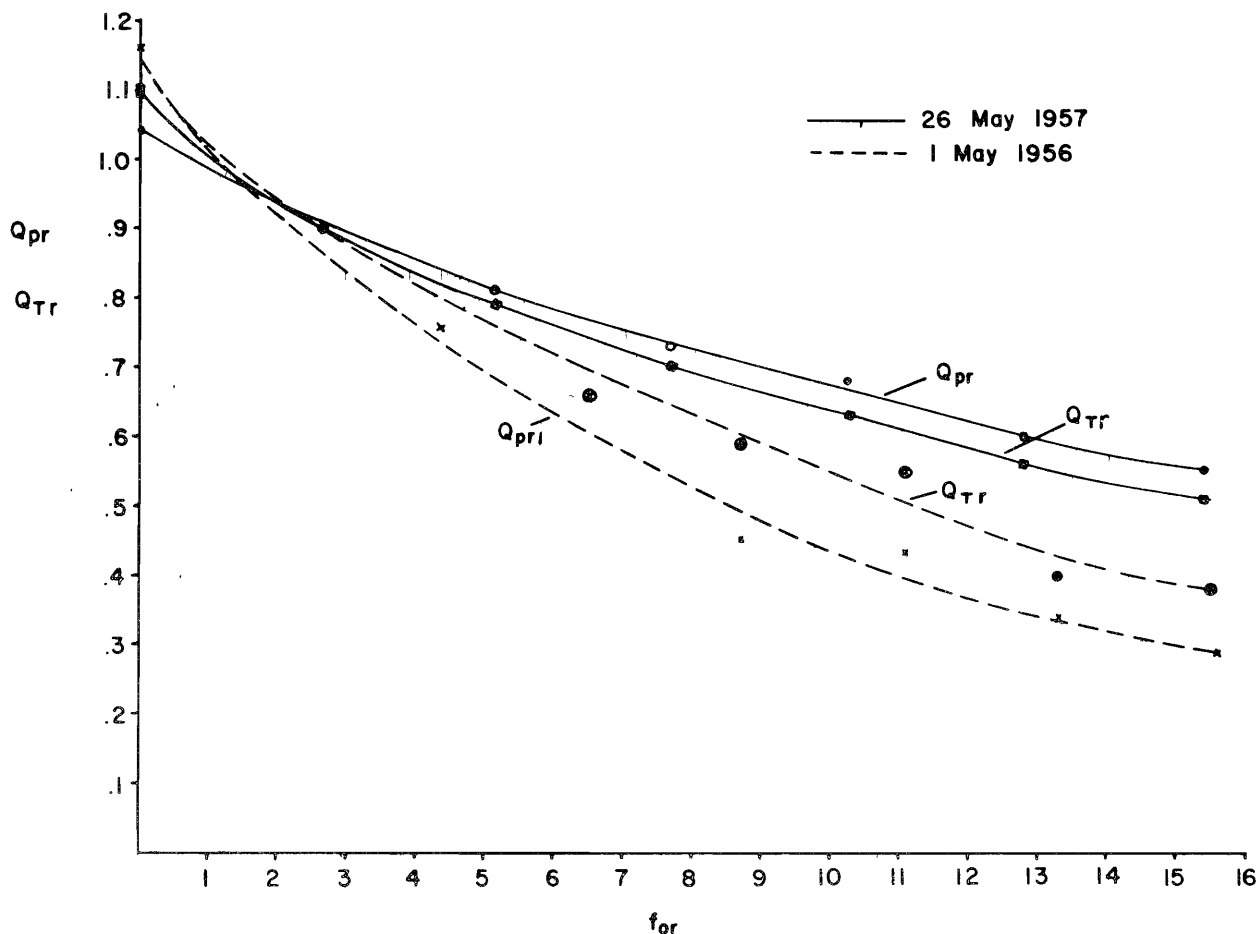


Figure 6.8. Variation in the ratios of the peak rate and total volume of outflow corresponding to the variation in the maximum infiltration capacity.

#### Minimum capacity infiltration rate

The values of  $f_c^{-1}/f_c$  or  $f_{cr}$  and the corresponding values of  $Q_p^{-1}/Q_p$  or  $Q_{pr}$  and  $Q_T^{-1}/Q_T$  or  $Q_{Tr}$  are presented in Table 6.22.

Figure 6.9 and 6.10 are the outflow hydrographs for the first and second storms under study for the various values of  $f_{cr}$  listed in Table 6.22. The relation between the  $f_{cr}$  and  $Q_{pr}$  on one hand and  $Q_{Tr}$  on the other are presented in Figure 6.11.

From these figures and the above data, it appears that the effect of varying  $f_c$  is more obvious on the second peak ( $Q_{p2}$ ) in a storm than on the first one. For the storm on May 1, 1956, the second peak is absent (Table 6.22) when  $f_{cr}$  is greater than 2.0. The total storm outflow is also affected significantly by variations in  $f_{cr}$ . This means that the minimum infiltration capacity is one of the important parameters that control the characteristics of the outflow hydrograph for this watershed.

#### Interception storage capacity

The significance of interception storage capacity on the outflow hydrograph characteristics is summarized in Table 6.23 and Figures 6.12, 6.13, and 6.14.

In Table 6.23,  $S_{Ir} = S_i^{-1}/S_i$ , and  $Q_{pr1}$ ,  $Q_{pr2}$ , and  $Q_{Tr}$  are defined before.

The effect of varying  $S_i$  on  $Q_p$  and  $Q_T$  seems to be significant. With reference to the first storm the effect of changing  $S_i$  ( $S_{Ir} = 3.34$ ) is more pronounced on the peak ( $Q_{pr1} = 0.26$ ) in the total volume ( $Q_{Tr} = 0.35$ ) than on the second peak ( $Q_{pr2} = 0.59$ ). This also is true in the case of the second storm. Variation of  $S_{Ir}$  has an inversely linear effect on the  $Q_{pr}$  and  $Q_{Tr}$  (Figure 6.14).

#### Depression storage capacity

Data showing the effect of  $S_D$  on the variation of  $Q_p$  and  $Q_T$  are presented in Table 6.24. The outflow

hydrographs for the various values of  $S_{D1}/S_{D0}$  or  $S_{Dr}$  are presented by Figures 6.15 and 6.16 for the first and second storms respectively. Figure 6.17 indicates the variation of  $Q_{pr}$  and  $Q_{Tr}$  for the corresponding values of  $S_{Dr}$  for both the storms. Both the data and the figures indicate that the relationships between (a)  $S_{Dr}$  and  $Q_{pr}$  and (b)  $S_{Dr}$  and  $Q_{Tr}$  are inversely linear (Figure 6.17). The effect of increasing  $S_{Dr}$  to 2 is to reduce the values of  $Q_{pr1}$ ,  $Q_{pr2}$ , and  $Q_{Tr}$  to nearly 0.6. When  $S_{Dr}$  is reduced below 0.64 in the range of 0.57 to 0.50, the effects on  $Q_{pr}$  and  $Q_{Tr}$  are not very pronounced (Figures 6.15 and 6.16). In this case the effect of  $S_{Dr}$  is equally significant on both the peaks and the total volume of outflow.

### Rise time of the unit hydrograph

The values of  $t_R^1/t_R$  or  $t_{Rr}$  and the corresponding  $Q_{pr}$  are presented in Table 6.25. There is no change in the value of  $Q_T$  for any change in the rise time  $t_R$ .

Outflow hydrographs resulting from various values of  $t_{Rr}$  are shown by Figures 6.18 and 6.19. Figure 6.20 presents the changes in the peak rate of outflow corresponding to variations of  $t_{Rr}$ . These figures indicate that the effect is more pronounced on the first peak ( $Q_{pr1}$ ) particularly when  $t_{Rr}$  is in the range of 0.6 to 2. With reference to Figure 6.20, for values of  $t_{Rr}$  greater than

Table 6.21. Maximum infiltration capacity and peak rate and total volume of outflow.

Date		$f_o^1/f_o = f_{or}$	$Q_p^1/Q_p = Q_{pr}$	$Q_T^1/Q_T = Q_{Tr}$
May 1, 1956	1	1.0	1.00	1.00
	2	.78	1.00	1.00
	3	.60	1.16	1.10
	4	2.22	.97	.97
	5	4.34	.76	.83
	6	6.50	.66	.66
	7	8.70	.45	.59
	8	11.10	.435	.55
	9	13.30	.34	.40
	10	15.60	.29	.38
May 26, 1957	1	1.00	1.00	1.00
	2	.85	1.00	1.00
	3	0	1.04	1.11
	4	2.56	.91	.90
	5	5.13	.81	.79
	6	7.69	.73	.70
	7	10.26	.67	.63
	8	12.82	.60	.56
	9	15.38	.55	.51
	10	20.51	.46	.43



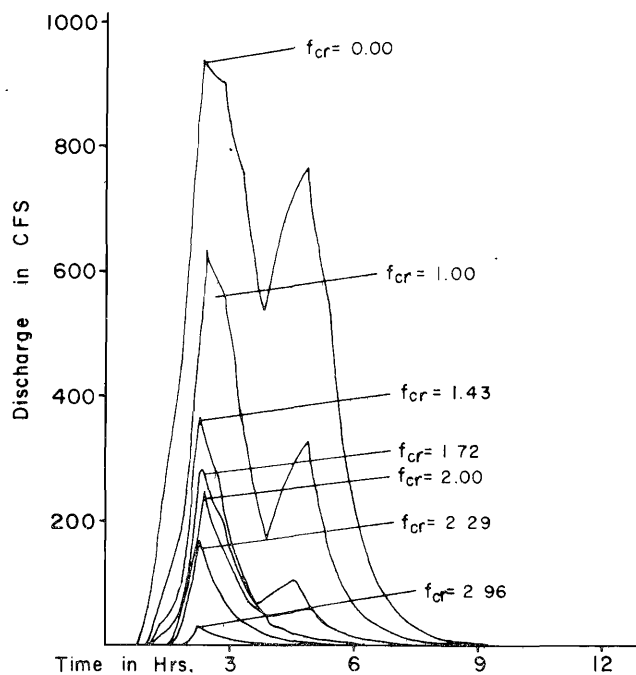


Figure 6.9. Outflow hydrographs resulting from the variation of  $f_c$  for the storm on 1 May 1956.

Table 6.22. Minimum infiltration capacity and peak rate and total volume of outflow.

Date	No.	$f_{cr}$	$Q_{pr1}^*$	$Q_{pr2}^*$	$Q_{Tr}$
May 1, 1956	1	1.00	1.00	1.00	1.00
	2	0.00	1.52	2.24	2.26
	3	2.96	.03	0	.02
	4	2.29	.26	0	.11
	5	2.00	.39	0	.20
	6	1.72	.45	.17	.35
	7	1.43	.58	.30	.42
May 26, 1957	1	1.00	1.00		1.00
	2	0.00	1.42		1.75
	3	2.02	.32		.21
	4	2.42	.50		.40
	5	2.12	.58		.49
	6	1.81	.73		.67
	7	1.52	.85		.84
	8	4.64	.02		.08
	9	3.64	.14		.15

\*  $Q_{pr1}$ ,  $Q_{pr2}$  refer to the first and second peaks occurring in the storm of May 1, 1956. For the storm of May 26, 1957, there is only one peak.

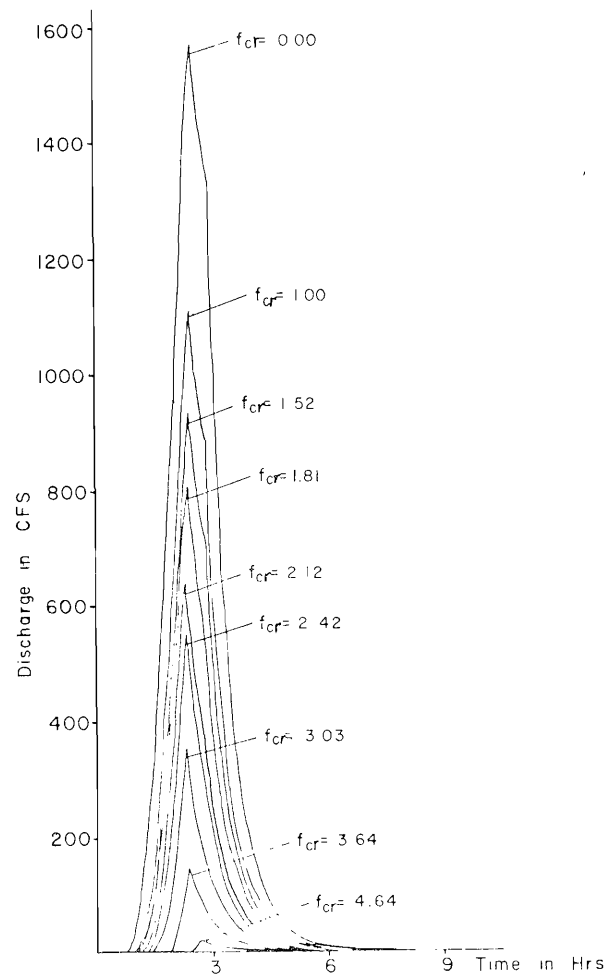


Figure 6.10. Outflow hydrographs resulting from the variation of  $f_c$  for the storm on 26 May 1957.

approximately 4.0, the model is relatively insensitive to changes in this parameter.

#### General comments

In general, the sensitivity studies reveal that the most significant parameters that affect the outflow hydrographs are  $f_c$ ,  $S_I$ ,  $S_D$ , and  $t_R$ . This implies that in model verification, their values should be carefully selected. Similar trends were obtained for both storms used in this analysis.

These results suggest that by extending the analysis to several storms non-dimensional relationships could be developed between the watershed coefficients and the peak rate and total volume of outflow.

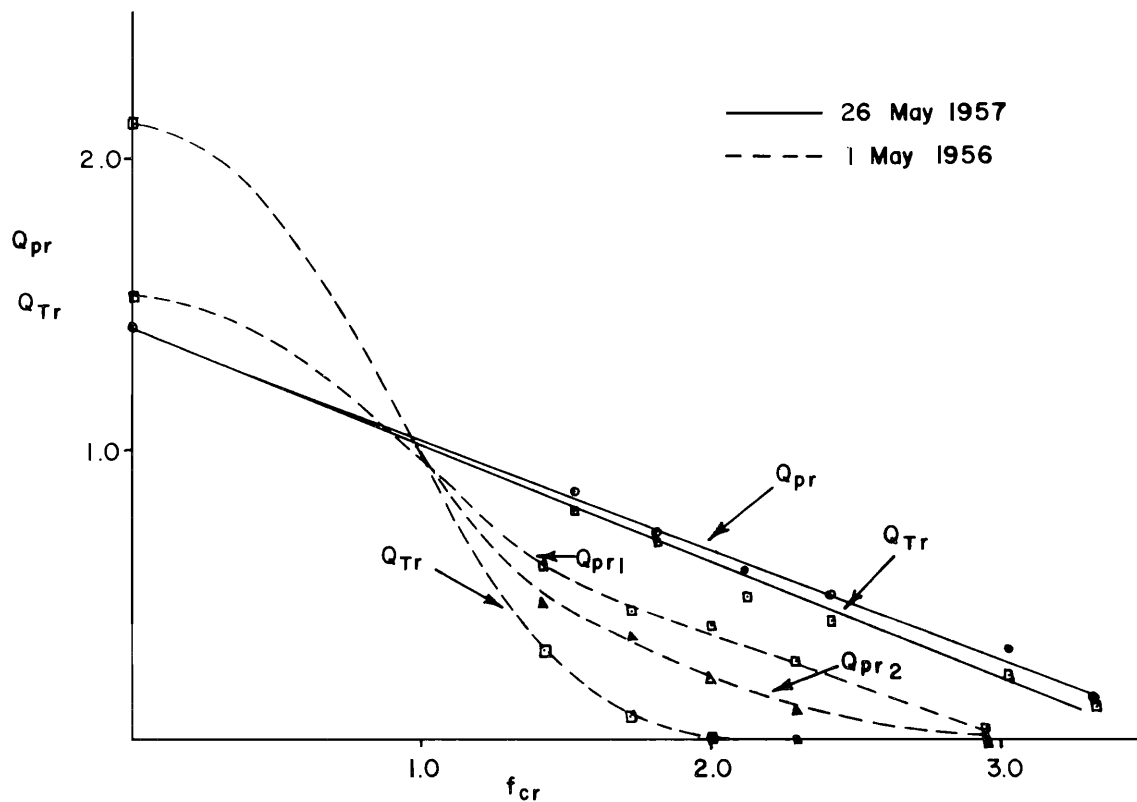


Figure 6.11. Variation of the peak rate and total volume of outflow corresponding to the variation in the minimum infiltration capacity.

Table 6.23. Interception storage capacity and peak rate and total volume of outflow.

Date	No.	$S_{Ir}$	$Q_{pr1}$	$Q_{pr2}$	$Q_{Tr}$
May 1, 1956	1	1.00	1.00	1.00	1.00
	2	1.67	.71	.88	.75
	3	3.34	.26	.59	.35
	4	.84	1.10	1.09	1.15
	5	.67	1.16	1.12	1.18
	6	.56	1.26	1.12	1.29
	7	.48	1.31	1.12	1.32
	8	.42	1.31	1.15	1.36
May 26, 1957	1	1.00	1.00		1.00
	2	1.69	.79		.79
	3	3.38	.35		.32
	4	.85	1.03		1.08
	5	.68	1.07		1.14
	6	.56	1.10		1.19
	7	.48	1.12		1.22
	8	.42	1.12		1.24

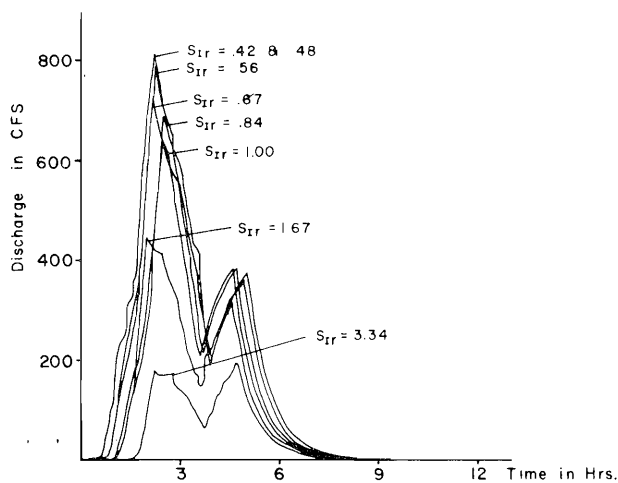


Figure 6.12. Outflow hydrographs resulting from the variation of  $S_I$  for the storm on 1 May 1956.

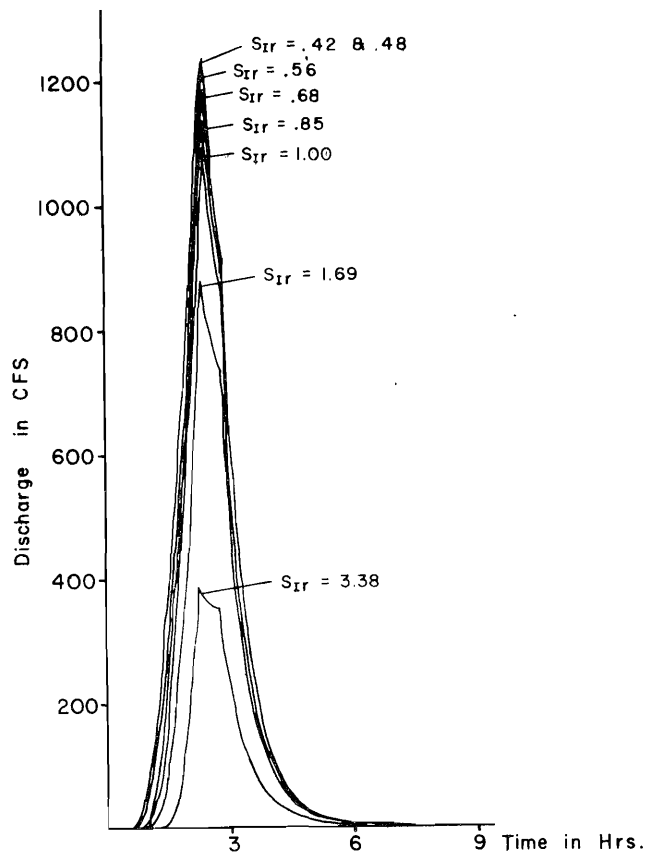


Figure 6.13. Outflow hydrographs resulting from the variation of  $S_I$  for the storm on 26 May 1957.

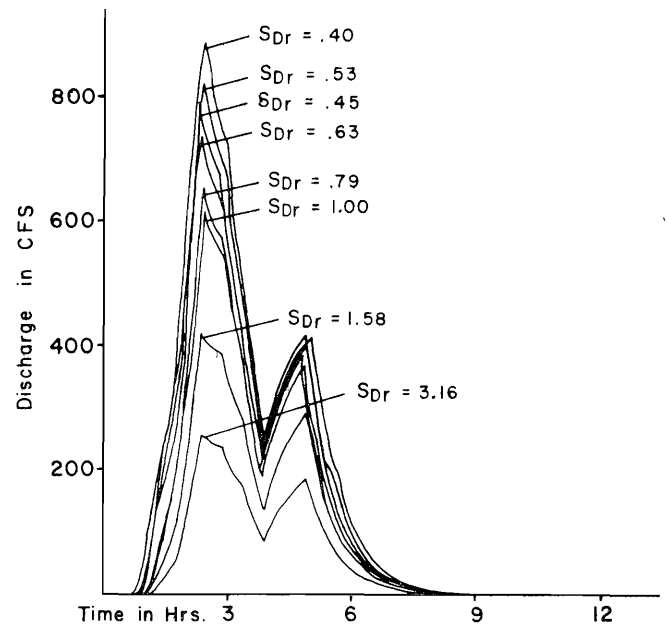


Figure 6.15. Outflow hydrographs resulting from the variation of depression storage capacity on 1 May 1956.

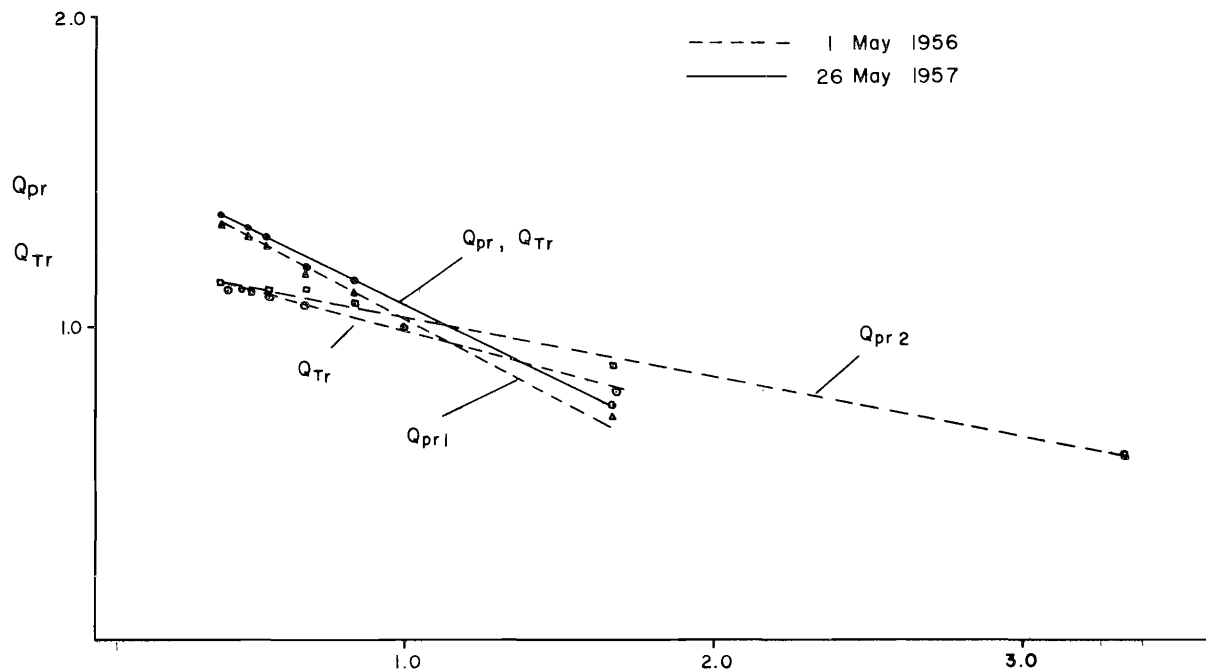


Figure 6.14. Variation of the peak rate and total volume of outflow corresponding to the variation in the interception storage capacity.

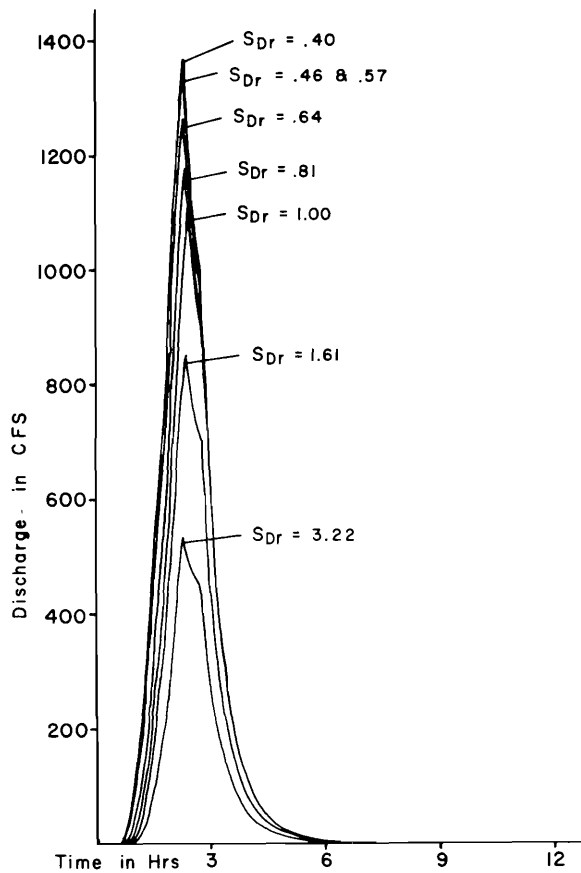


Figure 6.16. Outflow hydrographs resulting from the variation of depression storage capacity on 26 May 1957.

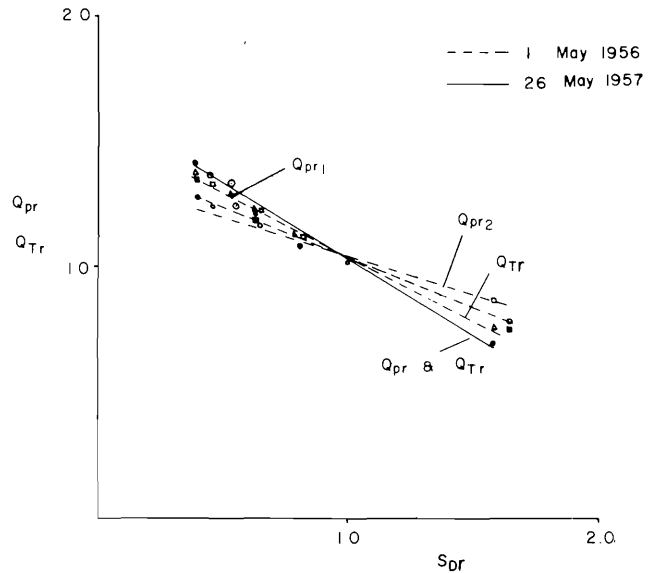


Figure 6.17. Variation of the peak rate and total volume of outflow corresponding to the variation in depression storage capacity.

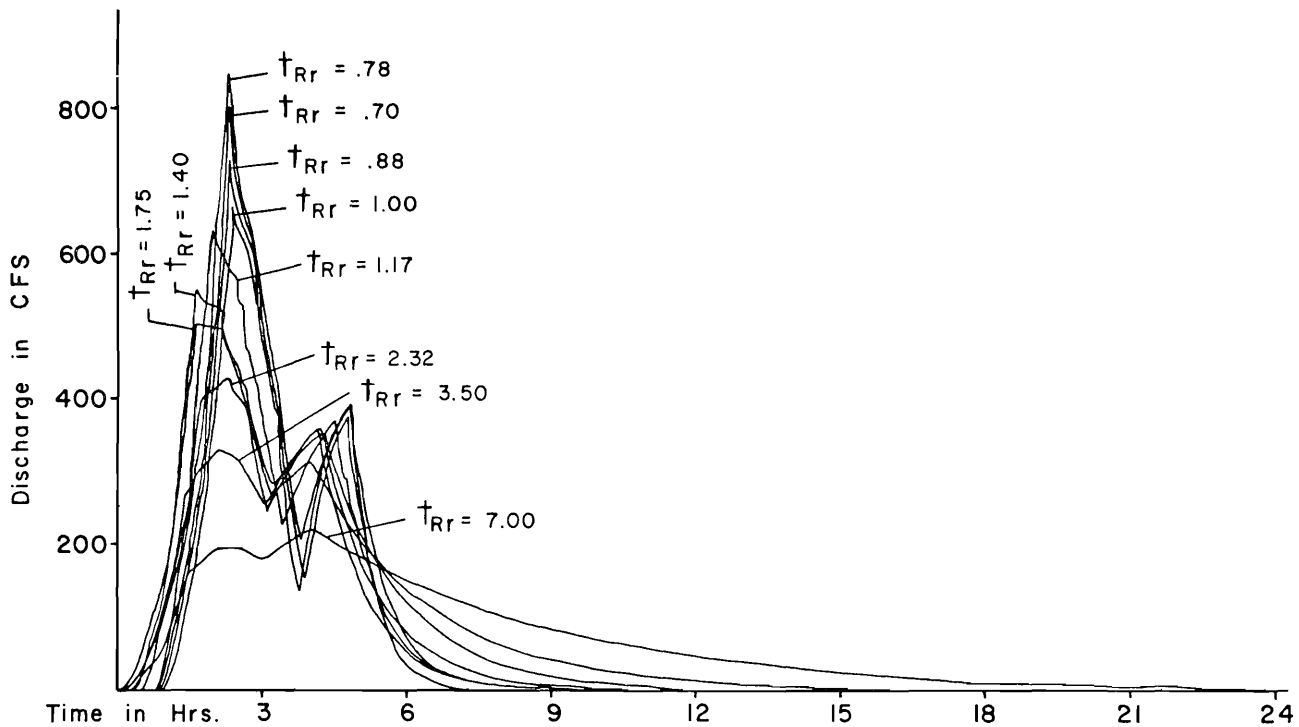
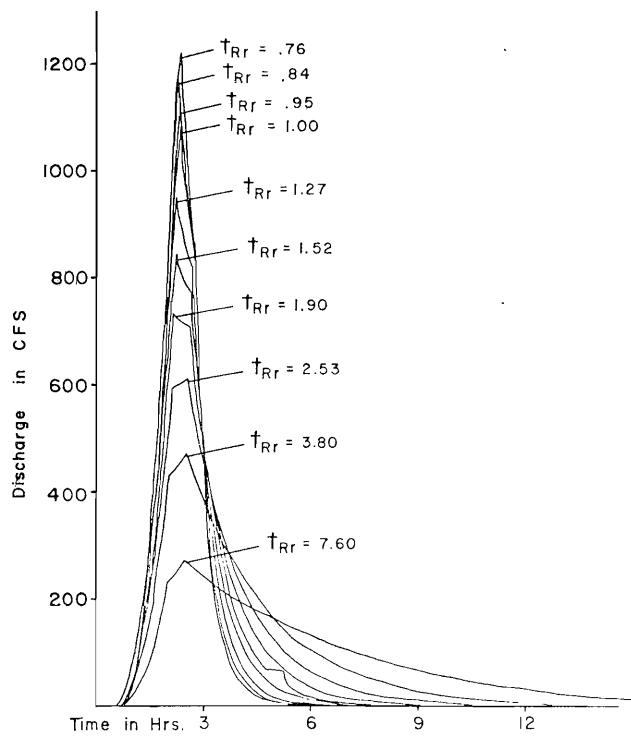


Figure 6.18. Outflow hydrographs resulting from the variation of the risetime of the unit hydrograph for the storm on 1 May 1956.



**Table 6.25. Rise time of the unit hydrograph and peak rate of outflow.**

Date	No.	$t_{Rr}$	$Q_{pr1}$	$Q_{pr2}$
May 1, 1956	1	1.00	1.00	1.00
	2	.88	1.09	1.05
	3	.78	1.18	1.11
	4	.70	1.24	1.13
	5	1.17	.91	1.05
	6	1.40	.80	1.00
	7	1.75	.74	1.00
	8	2.32	.62	.97
	9	3.50	.47	.86
	10	7.00	.29	.61
May 26, 1957	1	1.00	1.00	
	2	.95	1.02	
	3	.84	1.06	
	4	.76	1.11	
	5	1.27	.87	
	6	1.52	.76	
	7	1.90	.66	
	8	2.53	.55	
	9	3.80	.43	
	10	7.60	.25	

**Figure 6.19. Outflow hydrographs resulting from the variation of the rise time of the unit hydrograph for the storm on 26 May 1957.**

**Table 6.24. Depression storage capacity and the peak rate and total volume of outflow.**

Date	No.	$S_{Dr}$	$Q_{pr1}$	$Q_{pr2}$	$Q_{Tr}$
May 1, 1956	1	1.00	1.00	1.00	1.00
	2	1.58	.68	.85	.75
	3	3.16	.42	.56	.60
	4	.79	1.10	1.12	1.10
	5	.63	1.19	1.17	1.22
	6	.53	1.32	1.17	1.27
	7	.45	1.35	1.20	1.31
	8	.40	1.39	1.20	1.36
May 26, 1957	1	1.00	1.00		1.00
	2	1.61	.77		.78
	3	3.22	.49		.48
	4	.81	1.07		1.11
	5	.64	1.15		1.21
	6	.57	1.22		1.25
	7	.46	1.22		1.30
	8	.40	1.25		1.33

# 38TH STREET

SLOPE LENGTH AREA C1 C2

.009 23080.0 2.31 .2250 .0102

YEAR	AL	AL/L	PIC	LER	AER	AER1	AER2	AER3	AERM	SFR	TRU	THU	GPU	W50U	W75U
1950	9860.00	.4272	.2250	12236.	2.88	1.74	2.22	2.19	2.26	.01698	68.27	427.59	780.29	96.29	55.32
1951	10031.00	.4346	.2352	12047.	2.85	1.75	2.22	2.20	2.26	.01724	67.59	422.84	787.64	95.35	54.84
1952	10180.00	.4411	.2455	11836.	2.82	1.77	2.22	2.20	2.25	.01755	66.84	417.54	796.03	94.31	54.29
1953	10350.00	.4484	.2558	11682.	2.80	1.78	2.22	2.21	2.25	.01778	66.28	413.64	802.33	93.54	53.89
1954	10500.00	.4549	.2660	11509.	2.77	1.79	2.23	2.21	2.25	.01805	65.65	409.23	809.59	92.67	53.44
1955	10650.00	.4614	.2762	11350.	2.75	1.80	2.23	2.21	2.25	.01830	65.07	405.19	816.38	91.87	53.02
1956	10800.00	.4679	.2865	11205.	2.73	1.81	2.23	2.22	2.25	.01854	64.53	401.47	822.72	91.13	52.64
1957	10950.00	.4744	.2968	11072.	2.71	1.82	2.23	2.22	2.25	.01876	64.04	398.05	828.66	90.45	52.28
1958	11120.00	.4818	.3070	10980.	2.69	1.83	2.23	2.22	2.24	.01892	63.70	395.70	832.81	89.98	52.04
1959	11160.00	.4835	.3172	10702.	2.65	1.85	2.23	2.23	2.24	.01941	62.66	388.48	845.78	88.55	51.29
1960	11220.00	.4861	.3275	10470.	2.62	1.87	2.24	2.23	2.24	.01984	61.79	382.43	857.01	87.34	50.65
1961	11260.00	.4879	.3377	10223.	2.58	1.89	2.24	2.24	2.24	.02032	60.85	375.97	869.38	86.05	49.98
1962	11320.00	.4905	.3480	10019.	2.54	1.91	2.24	2.24	2.24	.02073	60.07	370.57	880.00	84.97	49.41
1963	11360.00	.4922	.3582	9799.	2.51	1.93	2.24	2.25	2.23	.02120	59.23	364.74	891.81	83.80	48.79
1964	11406.00	.4942	.3685	9600.	2.48	1.95	2.25	2.25	2.23	.02164	58.45	359.41	902.91	82.73	48.23
1965	11420.00	.4948	.3787	9370.	2.44	1.97	2.25	2.26	2.23	.02217	57.55	353.23	916.17	81.48	47.57
1966	11425.00	.4950	.3890	9141.	2.40	2.00	2.25	2.26	2.23	.02272	56.65	347.02	929.93	80.23	46.91
1967	11430.00	.4952	.3992	8923.	2.37	2.02	2.25	2.27	2.23	.02328	55.78	341.08	943.51	79.03	46.28
1968	11435.00	.4955	.4095	8716.	2.33	2.04	2.26	2.28	2.23	.02383	54.95	335.40	956.93	77.88	45.67
1969	11438.00	.4956	.4197	8517.	2.30	2.06	2.26	2.28	2.23	.02439	54.14	329.88	970.36	76.76	45.07
1970	11450.00	.4961	.4300	8337.	2.27	2.08	2.26	2.29	2.23	.02492	53.41	324.88	982.90	75.74	44.53

